Journal of Energy Storage 72 (2023) 108493

Contents lists available at ScienceDirect

Journal of Energy Storage

journal homepage: www.elsevier.com/locate/est

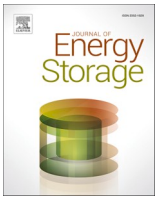

Review article

Enhancing safety in lithium-ion batteries with additive-based liquid electrolytes: A critical review

Robert Ilango Pushparaj [a], Ashish Ranjan Kumar [b], Guang Xu [a,*]

[a] Department of Mining and Explosives Engineering, Missouri University of Science and Technology, Rolla 65409, MO, USA
[b] Department of Energy and Mineral Engineering, Pennsylvania State University, 201 Old Main, University Park, PA 16802, USA

ARTICLE INFO

Keywords:
Li-ion battery
Electrolytes
Additives
Thermal safety
Electrochemical study

ABSTRACT

Lithium-ion batteries are widely used in various applications due to their high energy density, columbic efficiency, and scalability. While their safety mechanisms, such as heat-resistant separators, make them suitable for high-power devices, they require additional features when used in high-current and high-temperature systems. To address some of their inherent drawbacks, liquid electrolyte additives are increasingly being used in modern batteries. These chemicals, including borate, phosphate, nitrate, and phosphite, as well as polymers and other additives, can suppress the formation of the solid electrolyte interphase and dendrite layers, enhance thermal stability and useful life, and improve cycling characteristics. This paper provides an overview of the latest developments in contemporary additives and their significant contributions to battery efficacy. Additionally, the critical relationships between the thermal and electrochemical properties that impact battery safety are discussed.

1. Introduction

The rising energy demand requires secondary batteries with high endurance. Lithium-ion batteries (LIBs) are a popular choice for many electronic devices due to their high energy density and longer cycle life [1]. Research efforts have focused on enhancing their energy density and safety, enabling their use in electric vehicles (EVs) and electrochemical energy storage stations [2]. These efforts have included synthesizing anode and cathode materials, studying oxides and the elemental compositions, hybridizing with carbon and coating with various metal oxides, and doping with metals, which have all led to improved cycling stability [3]. Additionally, there has been a significant focus on improving battery separator safety by using novel polymers, ceramic coatings, and implementing porous materials. Moreover, formulation and development of new electrolytes have been emphasized to ensure safety and overall performance [4].

Battery electrolytes play a crucial role in ensuring the safety and optimal performance of LIBs across a wide range of usage conditions, including high temperatures, and varying voltages [5]. In addition, electrolytes are essential for enhancing ion conductivity and wettability. However, liquid electrolytes used in modern commercial LIBs, composed of Li-salts in non-aqueous solvents, can pose a significant risk of fire due to the flammability of the organic solvents [6]. Capacity decay and thermal runaway (TR) are the major threats. Traditional liquid additives exhibit high reactivity with Li-metal, leading to their rapid reaction with it and resulting in the formation of an unstable and non-uniform solid electrolyte interface. This, in turn, leads to the growth of Li-dendrites and presents safety concerns. The unmanageable development of Li-dendrite during the electrochemical procedure continues to pose significant challenges. This resulting in the utilization of liquid electrolytes forming a thicker solid electrolyte interface, thereby leading to diminished Coulombic efficiency and sub-par battery performance and longevity [7]. TR event starts when the battery's internal temperature rises due to overcharging, short circuits, thermal abuse, and mechanical damage, which could result in rapid combustion or explosion [8]. Therefore, it is essential to understand the properties of electrolytes and the design of the battery to mitigate the potential risks associated with LIBs and to improve their safety. Fires caused by batteries, accompanied by toxic smoke, pose a severe threat to the health of individuals affected and can even prove fatal in certain cases. Given their flammability, it is crucial to develop electrolytes that are resistant to fire and explosion. One effective approach to achieve this is by using electrolyte additives, which help render the electrolyte nonflammable while maintaining the high Coulombic Efficiency (CE) of the battery. The

* Corresponding author.
E-mail address: xuguang0530@gmail.com (G. Xu).

https://doi.org/10.1016/j.est.2023.108493
Received 27 March 2023; Received in revised form 21 July 2023; Accepted 23 July 2023
Available online 7 August 2023

addition of a small amount of electrolyte additive (typically 1.0–5.0 wt %) can significantly enhance battery performance at a low cost. According to previous reports, the addition of 1.0–5.0 wt% of an electrolyte additive has been found to greatly enhance battery performance. For instance, the inclusion of 1.0 wt% of tris (trimethysilyl) borate in a liquid electrolyte containing $LiPF_6$ was observed to exhibit excellent stability at temperatures of 30 °C and 55 °C [9]. Similarly, the use of an additive called tris (trimethylsilyl phosphate) at a concentration of 1.0 wt% in an electrolyte containing $LiPF_6$ demonstrated both thermal and cycling stability at 55 °C when paired with a $Li/LiNi_{0.5}Mn_{1.5}O_4$ [10].

There are several types of battery electrolyte additives, which can be classified based on their chemical composition as borates, phosphates, nitrates, phosphites, quercetin, imidazolide, polymers, and carbonates (Fig. 1). These additives react on the surface and form a protective film that enhances battery safety without affecting cycling performance. Moreover, some additives exhibit the ability to improve the thermal stability of the battery at elevated temperatures. Transition metal ions, such as Ni, Co, and Mn are commonly found in layered lithium-rich oxides. However, during the charge and discharge cycles of these oxides, these transition metal ions tend to dissolve in the electrolyte, which is typically carbonate-based. This dissolution leads to structural damage and a reduction in the capacity of the cathodes, negatively impacting the overall performance of the battery.

To overcome this drawback and improve the ionic conductivity of the electrolyte, various functional additives have been proposed. One example is the use of benzoic anhydride as a bifunctional electrolyte additive [11]. It serves as an interface between the cathode and the electrolyte, improving the overall performance of the battery. Additionally, it also has the capability to capture gases that may be generated during battery operation, further enhancing safety.

Another multifunctional additive that has been investigated is ethoxy (pentafluoro (cyclotriphosphazene)) [12]. This additive plays a crucial role in enhancing the conductivity of the electrolyte by reducing charge transfer resistance. It also helps suppress undesirable side reactions without sacrificing the cycling performance of the battery. Furthermore, Resorcinol bis(diphenyl phosphate) (RDP) has been suggested as a bifunctional electrolyte additive [13]. Its primary role is to enhance the safety of the battery by reducing the extinguishing time. By incorporating RDP into the electrolyte, the overall safety of the battery can be improved, making it less prone to fire hazards.

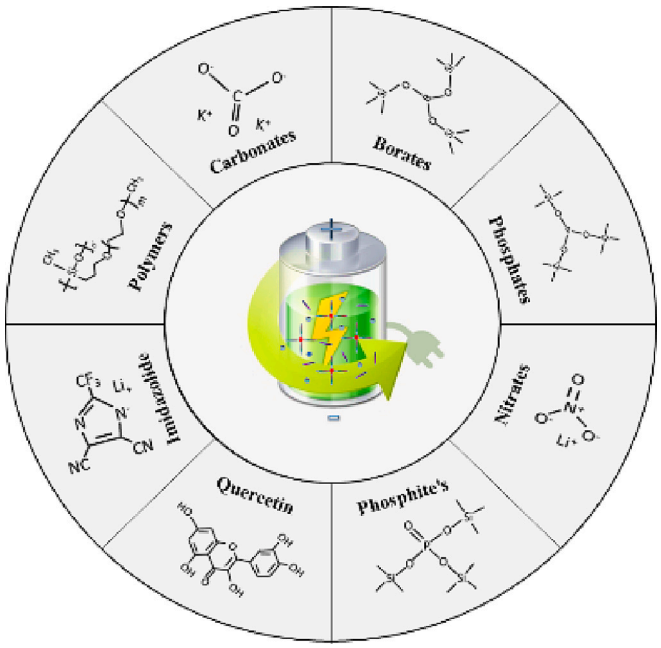

Fig. 1. Different functional additives for Li-ion battery applications.

This review paper critically examines the thermal stability and properties of additive-based electrolytes for the development of next-generation safe LIBs. It offers valuable insights into the current progress and challenges associated with the synthesis of these liquid electrolytes, along with their risk analysis under harsh conditions. The review article is structured into seven sections, with Sections 2–4 focusing on the structure, functional groups, cycle lives, and high-temperature performance of commonly used additives. Section 5 discusses the contributions of other additives, including organic quercetin, amide imidazolide, polymers such as poly-siloxane-g-ethylene oxide, and inorganic salt carbonates towards enhancing the safety of LIBs. Finally, the review paper concludes by summarizing the current state of additives and outlining the necessary technology to develop the next generation of electrolyte systems that will further improve the safety of LIBs.

2. Borate additives

Borate-based additives are used to enhance battery safety and stability. They were studied under high temperatures and found to maintain the thermal stability of the battery. Research has shown that their unique qualities including their molecular structure enhance their thermal stability. For example, Sun et al. reported the boron-based anion receptor tris(pentafluorophenyl) borane (TPFPB) could control the thermal decay of a $LiPF_6$-based electrolyte [14]. $Li/LiMn_2O_4$ cells using TPFPB additive exhibited superior capacity retention and cycling efficiency at 55.0 °C. There was also a significant increase due to the enrichment of $Li^+PF_6^-$ ion-pair separation. The comparative analysis with and without additives is illustrated in Fig. 2(a), which also demonstrates the influence of borate additives against the severe HF attack. Fig. 2 (b) depicts the model of the SEI structure in the FEC electrolyte with and without additives on the negative electrode surface [15]. The additives result in the formation of a protective layer on the electrode surface leading to safe LIBs with improved cycle life.

Another widely used boron-based additive is tris(trimethylsilyl) borate (TMSB). Liu et al. reported that 5.0 wt% of TMSB added to the electrolyte (EC/DMC with 1.0 M $LiPF_6$) resulted in significant capacity retention improvement at temperatures up to 55.0 °C [16]. They used $LiMn_2O_4/Li$ half cells to test the thermal stability of the battery. In addition, storage tests were run for 24, 48, and 72 h at 80.0 °C to study the full charge status. After long-term cycling, the X-ray photoelectron spectroscopy (XPS) study revealed the peak intensity and position that controls the surface chemistry. The intensities of C—H and C—O bonds detected on the surface of the $LiMn_2O_4$ electrode after cycling with the TMSB additive were much greater than without the additive. The TMSB forms as $R—CH_2OCO_2—Li$ on the $LiMn_2O_4$ surface which ensures stability and fast Li-ion diffusion. Likewise, $Li/LiFePO_4$ battery was proposed with 1.0 wt% of TSMB at 55.0 °C resulting in higher discharge retention of 94.0 % compared to 76.0 % observed without additive. Similarly, the cycling stability over 80 cycles was noted with reduced capacity decay at high temperatures [9].

TSMB additives have been used in both half-cell and full-cell systems which indicates their suitability for different types of battery systems. For instance, high voltage materials like $Li/LiNi_{0.5}Mn_{1.5}O_4$, with a high specific capacity (146.7 mAh g^{-1}) have been studied with TSMB with the tuning of additive starting from 0.2 to 2.0 wt%. Notably, over 200 cycles, the prepared battery with 1.0 wt% TMSB has excellent cycling properties along with 95.3 % capacity retention. This is higher than the cell with standard electrolyte (84.4 % capacity retention). The high-temperature storage study (60 °C) for one week at a fully charged state demonstrates a discharge capacity of 122.1 mAh g^{-1} with additive and 109.9 mAh g^{-1} without additive which indicates the thermal stability of TMSB [17].

Borate additives were studied at room temperature for their cycling and other electrochemical properties, such as rate capability, kinetics, and electrochemical impedance. Also, the high-voltage materials along

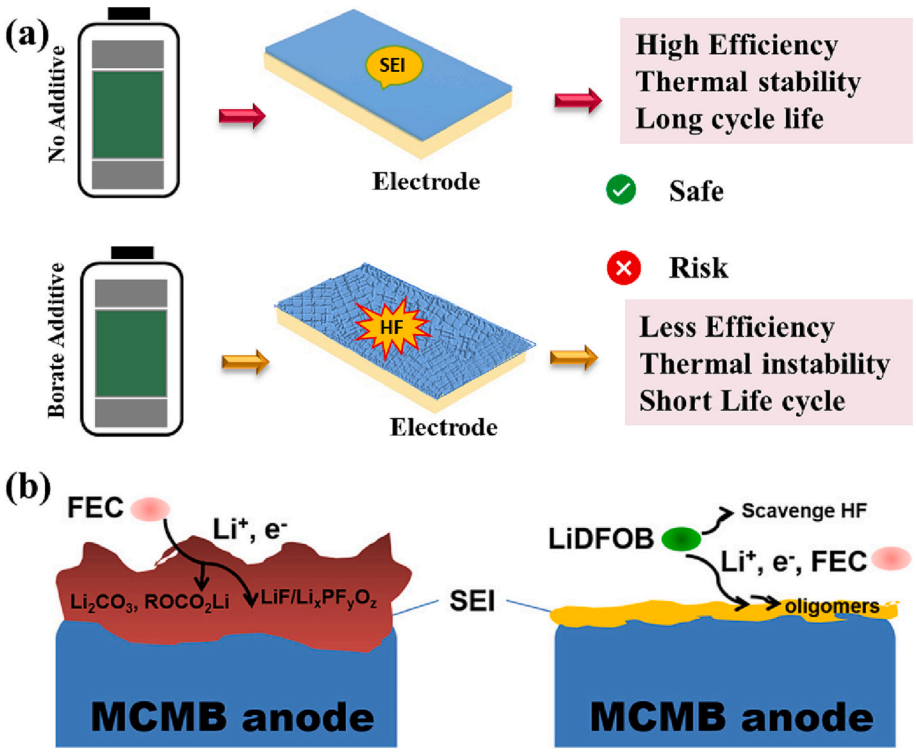

Fig. 2. Borate additives' characteristics for Li-ion battery (b) SEI structure in the FEC-based electrolyte with and without additive. Reproduced with permission copyright (2017) ACS [15].

with TSMB were extensively studied to explore the impact of additives. Zuo et al. evaluated the battery performance between 3.0 V and 4.4 V with $LiNi_{0.5}Co_{0.2}Mn_{0.3}O_2$/graphite model [18]. In this study 0.5 wt% of TSMB shows a higher initial discharge capacity of 181.0 mAh g^{-1}. It maintained retention of about 92.3 % after 150 cycles, which is lower than the 1.0 wt% that was reported in the previous literature [17]. TMSB-containing electrolyte added at 0.5 wt% maintains the crystal integrity. These additive forms a uniform thin layer of about 10 nm thickness which improves the Li $[Li_{0.2}Mn_{0.54}Ni_{0.13}Co_{0.13}]$ O_2 cathode's interfacial stability that results in suppressed electrolyte decomposition [19]. Remarkably, the CE of the TSMB-containing electrolyte (97.8 %) is slightly higher than the standard electrolyte (97.2 %), corroborating the structural stabilization of Li-rich materials.

The TMSB additives effect may be evaluated by introducing different types of Li-intercalated cathode materials with unique operating potentials. For example, $LiNi_{1/3}Co_{1/3}Mn_{1/3}O_2$ cathode material can operate at a high voltage of up to 4.5 V. However, at 4.5 V, the cathode structure faces severe structural deterioration due to metal ion dissolution and HF reaction. Liao et al. used TMSB against Li/$LiNi_{1/3}Co_{1/3}Mn_{1/3}O_2$ and reported that 1.0 wt% of the additive exhibits 79.7 % CE in the first cycle. This is lower than the cell without the additive. There are two possible reasons for low CE: (i) decomposition of electrolyte at 4.5 V, and (ii) occupation of Li-sites by Ni during the charge-discharge process. After the first cycle, the CEs with and without the TSMB additive were about 98.8 % and 97.5 %. This difference could be due to the high interfacial contact [20]. Similarly, 1.0 wt% TSMB shows a better protective layer on $LiCoPO_4$ under 5.0 V [21]. After the 50th cycling, the SEI film formation and thickness were identified by the SEM and TEM analysis. The surface morphology after cycling exposed the thickness of the coating layer (about 20.0 nm) by 1.0 wt% of TSMB, suggesting a thin surface film effectively increases battery performance.

Notably, borates with different functional groups were also found to be an alternative additive to improve the battery capacity and cycling of high-voltage electrodes. Liu et al. tested trimethyl borate (TMB) additive without silyl group with the Li/$LiCoO_2$ system. The 2.0 wt% TMB additive showed capacity retention of about 81.0 %. A 25.0 nm layer was formed on the surface that prevented electrolyte decomposition, which was confirmed by the XPS analysis and followed by deconvolution of the C—F spectrum [22]. Similarly, some additives like triethyl borate (TEB), trimethylboroxine, and tributyl borate (TBB) were proposed. These are added in 1.0–10.0 wt% and improve different rate capacities, cycling life, CE, and battery stability [23–25].

Salt-based borate combination may offer better results than commercial $LiPF_6$-based electrolytes. Li salt-based additives not only lower the decomposition of ethylene carbonate (EC), propylene carbonate (PC), and other solvents on the electrode but also increase the rate capability, cycling life, and cell safety. Lithium bis (oxalate) borate (LiBOB) salt is recommended as an additive for its favorable electrochemical and thermal properties with graphite when combined with different cathodes. For example, Asruf et al. used LiBOB salt and studied various aspects of surface film chemistry at 350.0 °C. This study was performed at high potential charging and discharging of cells. This showed electrode stability at high potential and high thermal stability over 350.0 °C [26]. Later, Wang et al. theoretically predicted that LiBOB salt has a higher oxidation reaction which helps to increase the solvent decomposition rate due to charge distribution, resulting in long cycling life [27]. To support this mechanism, Pieczonka et al. used LiBOB additive along with the $LiNi_{0.42}Fe_{0.08}Mn_{1.5}O_4$/Li half cells and $LiNi_{0.42}Fe_{0.08}Mn_{1.5}O_4$/graphite full cells [28]. A concentration of 1.0 wt% added LiBOB in the electrolyte significantly improved the battery performance during the half-cell testing. In a further study with a full-cell system, the capacity retention with the additive concentration of 1.0 wt% was slightly higher than 3.0 wt% at 30 °C. To understand more about the impact of LiBOB on electrolyte stability, the 1.0 wt% electrolyte additive was used to operate the full-cell battery at 45 °C. Remarkably, 1.0 wt% LiBOB demonstrated 95.0 % capacity retention which is incomparable to the pristine electrolyte. This could be due to three major reasons, (i) reduction of dissolved Mn, (ii) formation of passivation film formation on the electrode surface, and (iii) capture of PF_5 free radicals. Moreover, TEB additives revealed good retention

(99.0 %) after cycling as mentioned (see Fig. 3), comparing all borate-based additives and the effect of different quantities shows that additive optimization is crucial to maintaining stable and safe LIBs.

2.1. Guidance for development of new borate additives

When selecting boron-based additives, it is important to consider the anion receptor that will regulate the solvation and diffusion of Li-ions in the ethylene carbonate electrolyte. For instance, super halogen additives can decrease the self-association of Li-ions and the formation of Li^+ PF_6^- ion pairs. This, in turn, facilitates Li-ion transport and reduces solution viscosity. Additionally, the quantity of additives has a significant impact on the solid electrolyte interphase (SEI), which can dissolve LiF from the SEI on the cathode, leading to decreased interfacial resistance. Furthermore, the thermal stability of borate additives plays a crucial role in enhancing the SEI and battery performance. It is essential to select additives that remain stable at temperatures exceeding 55 °C for at least 100 cycles while maintaining a slow current rate of less than 0.5C. Finally, employing borate additives enables the formation of a thin and stable cathode-electrolyte interface (CEI) layer, ideally measuring less than 10 nm.

Before incorporating borate additives into LIBs, it is crucial to thoroughly understand their film-forming mechanism, gas-releasing principle, and oxidative stability. This understanding is vital due to the close relationship between the oxidative decomposition of the electrolyte on the cathode surface and the associated safety risks. By shedding light on these aspects, it can be ensured that the borate additives selected for use in LIBs are compatible with the battery system and do not pose a significant safety hazard. Considering these factors is crucial when choosing new additives for rechargeable LIBs.

3. Phosphates and phosphite additives

Phosphate-based additives are suitable chemicals that could result in the alleviation of LIBs battery fire risk. They show excellent thermal stability and cycling performance at room and high temperatures. Fig. 4 describes the role of phosphate-based additives against undesirable chemical reactions. They act as shields, thus extending their useful life. Phosphate-based materials, used widely in the plastic manufacturing industry as flame-retardants, are added to the LIB electrolytes to suppress flammability and improve their safety. In a pioneering work, Wang et al. studied the fundamental characteristics of phosphate solvent with electrolytes and reported that 1.0 mol/dm^3 ensures nonflammability

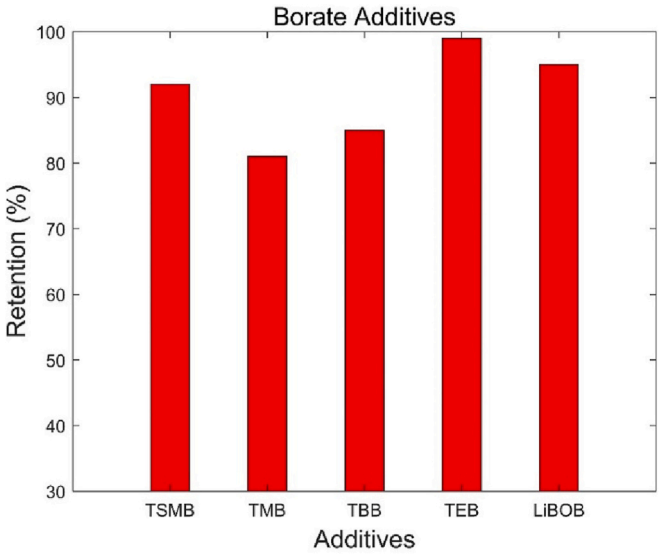

Fig. 3. Capacity vs. retention profiles of different borate additives.

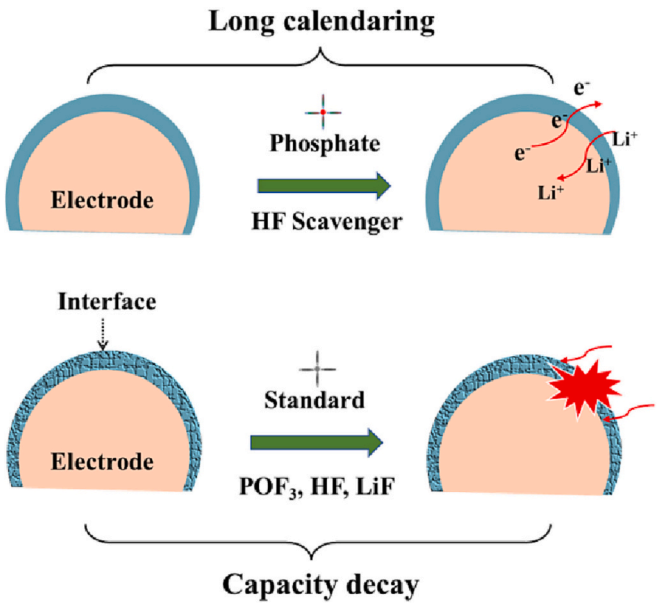

Fig. 4. Phosphate additives' characteristics for Li-ion battery.

due to the co-solvent boiling point and generation of hydrogen radicals [29]. Their thermal stability was measured by conducting a DSC analysis. The $NG_7/LiCoO_2$ cell showed better stability after adding trimethyl phosphate (TMP). The same research group further introduced phosphate-based TMP electrolytes against amorphous carbon/$LiCoO_2$. This non-flammable electrolyte exhibits notable cycling performance over 30 cycles. Additionally, this electrolyte was also observed to have good performance even at −40 °C [30]. Further, the thermal stability investigation findings revealed that the phosphate composition of 1.0 mol/dm^3 $LiPF_6$/EC: PC: DEC: TMP (30:30:20:20) demonstrated very good thermal stability at the 90.0 % charged state. Additional tests at temperatures showed that the TMP-based electrolyte is safe at high temperatures as well as extremely low temperatures.

The additives' concentration affects the battery's thermal, electrochemical, and interfacial stability. Experimental and analytical tools have established that the high ~20.0 wt% TMP concentration significantly improves the battery performance [30]. To evaluate the TMP nonflammability, Ota et al. added ethylene ethyl phosphate to TMP during the electrolyte preparation. Graphite anode soaked in 1.0 mol/dm^3 $LiPF_6$/EC + PC + DEC + TMP + EEP 5.0 % did not exhibit a CO_2 peak which indicates their thermal stability. This results from stable SEI formation and electrolyte decomposition at high temperatures (110 °C) [31]. Research has reported that TMP-based electrolytes with high concentrations exceeding 70.0 % enhance LIB safety. Furthermore, the graphite anode had a high discharge capacity (352.0 mAh/g) with a high CE of 99.5 % attributed to the high flash point of cosolvent mixing [32]. The performance of TMP at high temperatures was examined by subjecting different activation processes at 55 °C with a $LiCoO_2$/MAG10 full cell. This excellent rate capability performance is due to the stable formation of SEI, observed from a cyclic voltammetry test, and decomposition suppression of electrolytes by the MP additive [33].

Flammability tests have upheld the phosphate-based additives' suitability for safe LIB operations. They show non-flammability qualities at high temperatures. Tris(trimethylsilyl)phosphate (TMSP) additive, for example, forms a surface-modified SEI on many electrode materials including graphite anode, layered, Li-rich, and Ni-rich cathode material in LIBs. TMSP additives overall protected all electrode surfaces and improved battery performance. For example, J. Zhang et al. used 1.0–2.0 wt% TMSP with electrolyte during the Li $[Li_{0.2}Ni_{0.13}Mn_{0.54}Co_{0.13}]O_2$/Li cell preparation [34]. The cell performance was studied in the 3.9–4.4 V range. This showed higher capacity

retention of 91.1 % over 50 cycles at 1.0 wt% of TSMP. It maintained 225.0 mAh/g capacity due to an SEI layer formation that was verified by XPS intensity interpretation of C1s and F1s peaks. However, thermal studies were not conducted in this research. Later, the TMSP was used to increase the cyclability of $Li/LiNi_{0.5}Mn_{1.5}O_4$ cells. The cells were used in high voltage (4.9 V) at room (25 °C) and elevated temperature (55 °C). The cycling test showed that continual electrolyte decomposition stopped or was delayed upon prolonged cycling on the addition of 1.0 wt % TMSP. The CV test verified the fast electrode kinetics of the high redox current, achieving 94.9 % capacity retention after 70 cycles at high temperatures [10]. Later, Rong et al. also used 1.0 % wt TSMP in the $Graphite/LiNi_{0.4}Co_{0.2}Mn_{0.4}O_2$ full cells system operating at 4.35 V and reported a discharge capacity retention of 90.8 % after 70 cycles [35]. This result seems inadequate to make conclusive decisions since only 70 cycles were reported. However, 1.0 wt% TSMP used in the $LiNi_{0.4}Co_{0.2}Mn_{0.4}O_2$ half-cell showed a capacity retention of 90.9 % at 1C (C representing the current rate). Further, this study strongly suggests the growth of an amorphous SEI layer on the surface of the cathode that protects it from HF after 100 cycles. This suggests that TSMP works with both full-cell and half-cell systems [36].

Although 1.0 wt% TSMP shows comparable discharge capacity retention for Ni-rich cathode materials, research shows that it can be varied from cathode to cathode and anode to anode due to structural chemistry and stability. For example, $LiNi_{1/3}Co_{1/3}Mn_{1/3}O_2$ showed a retention of 92.3 % in the first cycle with 160.5 mAh/g after adding 1.0 wt% TSMP. The charge-discharge profile suggests that TSMP not only protects the surface but also hinders the structural destruction of electrode materials [37]. Ren et al. examined the electrochemical performance of an anode with 5.0 vol% TSMP additive at a high temperature and showed a life exceeding 70 cycles with a retention of 96.1 %. The charge transfer resistance studies showed a conductivity increase after adding the 5.0 vol% TSMP, although the performance depends on the electrolyte solution [38,39]. Other cells with phosphates-based flame-retardant additives like Triphenylphosphate (TPP) are stable up to 5.0 V. Moreover, it helps to improve the LIB's thermal stability. When adding TPP to the electrolyte solution, the cells release significantly less heat. For example, Hyung et al. verified the thermal stability of TPP using CV analysis and showed its stability up to 5.0 V. In addition, it shows notable safety features in the 2.5–4.3 V range. The ARC study shows that less than 5.0 wt% TPP increases the onset reaction temperature from 160.0 °C to 210.0 °C. The lower heat release enhances LIB safety [40]. Moreover, the flame propagation rate profile shown in Fig. 5 shows that 5.0 wt% is the optimum concentration that reduces the flame rate significantly. Further onset temperature and thermal runway tests conducted by Doughty et al. using 18650 cells and ARC techniques showed remarkable changes in the in-gas emission [41]. But they did not provide enough data to support the relationship between thermal stability and electrochemical characteristics. Shim et al. studied TPP as an additive to determine the relationship between thermal and electrochemical behaviors using CV, DSC, and charge-discharge studies. The optimized 3.0 % TPP additive improved the high voltage performance up to 4.9 V which is a higher voltage than the previous reports. Finally, this research showed that this electrolyte synthesis consists of a trade-off between the thermal stability of the electrolyte and cell characteristics. Also, this type of additive acts in the condensed phase, promoting char growth on the surface thus protecting the surface of the electrode [42].

Phosphate electrolytes were studied with functional additives for their thermal and electrochemical properties. They were observed to enhance the LIB stability. For instance, the diphenyloctyl phosphate (DPOF) additive was analyzed for its thermal stability using the DSC analytical instrument. In this study, a 5.0 wt% DPOF was used in $LiPF_6$/EC: EMC, and reaction peaks were studied. The peaks at 215.0 °C with DPOF were lower than the peak located at 235.0 °C without DPOF suggesting its efficacy [43]. However, this study lacked in-depth charge-discharge studies at elevated temperatures, which could be indispensable for commercial applications. Afterward, the phosphazene electrolyte additive was studied with cylindrical batteries. The flammable test confirmed its stability up to 200.0 °C [44]. Furthermore, the overcharge test had been conducted at voltages exceeding 10.0 V which is higher than previous LIBs research.

Thermal heating tests using a burner showed the self-extinguishing properties of the phosphate electrolytes during venting. These results imply that electrolytes with phosphazene-based flame retardants could be used to make safe LIBs. Subsequently, nonflammable dimethyl methyl phosphonate (DMMP) was shown to be a thermally stable additive. The spinel or olivine-based cathode giant alloys were used. The ball mill technique was used to ensure a uniform particle size for this study. Olivine-based materials with DMMP and 10.0 % of FEC additive maintained stable cycling over 150 cycles during this research. Essentially, the thermal test revealed that $SiO/LiFePO_4$ in the 0.8 M $LiPF_6$

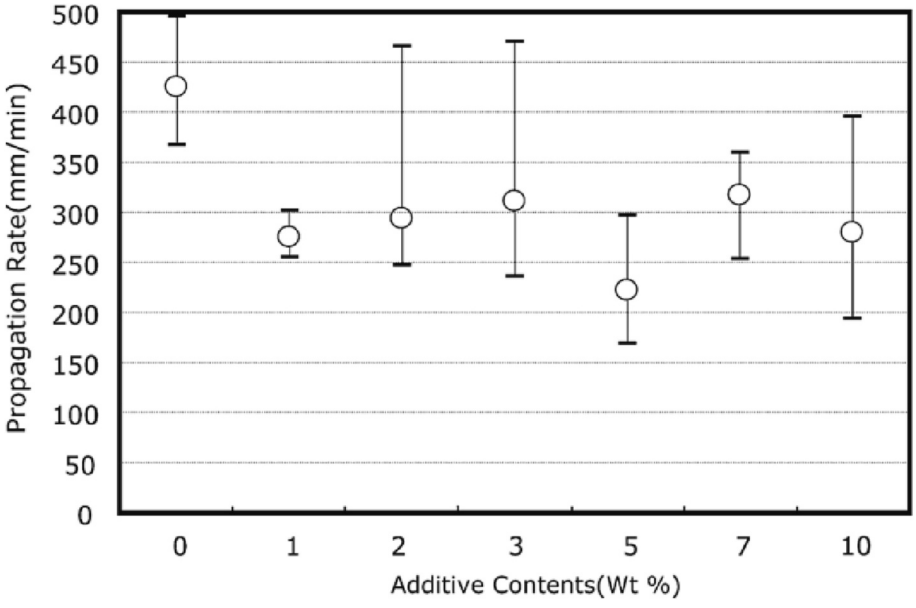

Fig. 5. Flame propagation of test for different additives.
Reproduced with permission copyright (2003) Elsevier [40].

DMMP + 10.0 % vol FEC shows almost no exothermic reactions in the 25.0 °C–180.0 °C temperature range. This implies that the DMMP electrolyte has very high thermal stability even on the surface of the charged cathode [45]. Therefore, these materials can be used in large-scale format batteries for future safe energy storage applications.

Ethoxy(pentafluoro) cyclotriphosphazene (PFPN) is a supplemental flame retardant electrolyte additive and can be used as multifunctional material. Studies by Li et al. using 5.0 vol% of PFPN showed a self-extinguishing time (SET) of 12.38 sg^{-1} and a critical oxygen index (COI) of 22.9, without conceding the capacity of the cathode [46]. After adding the PFPN, the initial discharge capacity was about 150.7 mAh g^{-1}, with a capacity retention of 99.14 % after 30 cycles at 0.1C in the $LiCoO_2$ battery. Additionally, the electrode polarization was reduced, and the low-temperature activity was improved. Likewise, Xu et al. carried out the flammability test followed by long-term cyclability on fluorinated alkyl phosphate additive [47]. The impact of fluorine addition showed high flame suppression and ion transport that helps safe and efficient LIBs. This could happen due to the following reasons: (i) the optimized content of fluorine, (ii) the combined effect of fluorine and phosphorous groups, and (iii) the formation of stable SEI by organo-fluorine in carbonate molecules. Further, the improvement of the cathode electrolyte interface (CEI) and electrolyte decomposition products like LiF, $Li_xPO_yF_z$, and Li_2CO_3 was investigated using XPS analysis with another fluorinated phosphate. Lithium bis(2,2,2-trifluoroethyl) phosphate (LiBFEP) additive was used in $LiPF_6$ in EC/EMC 3:7 wt% in which the additive content was 0.1 and 0.5 wt%. This study proposed that the growth of the CEI alleviates electrolyte oxidation and stops the decomposition of $LiPF_6$. Also, it averts HF-induced manganese (Mn metal) dissolution from the cathode and destabilization of the SEI, which helps with capacity retention and coulombic efficiency after long-term cycles [48].

Compared to the 0.1 wt%, the 0.5 wt% additive shows significant improvement in ICE (87.0 %) and capacity retention (79.0 %) after 190 cycles at a current rate of C/5. The operation potential ranged from 3.3 V to 4.8 V. Similar fluorinated phosphate additives electrolyte stable up to 5.0 V were researched by Cresce. A new class of tris(hexafluoro-isopropyl) phosphate was synthesized via solution mixing, in which 0.45 mol 1,1,1,3,3,3,3 hexafluoro-2-proponal, diethyl ether and lithium hydride, lithium chloride, and $POCl_3$ were used with about 1.0 wt% additive concentration. The $LiNi_{0.5}Mn_{1.5}O_4$ cathode provides a capacity of 108.0 mAh/g with this fluorinated electrolyte additive which is better than 98.0 mAh/g without the additive [49]. Since this was preliminary data, further research is required to determine the performance in a harsh environment. On the other hand, lithium difluoro phosphate ($LiPO_2F_2$) is proposed as an SEI stabilizer due to its unique molecular properties. Interestingly, with this $LiPO_2F_2$ additive (1.6 wt%), cycle performances of $LiCoO_2$/graphite (model 18650) batteries show 88.6 %, which is much greater than the standard 75.7 %. Additionally, this cell was very stable even after 2400 cycles at a 1C rate [50]. Compared to previous fluorinated/phosphate-based additives, this is the highest reported cycle count. Another electrolyte additive is lithium dimethyl phosphate (LiDMP), which was tested along with NCM/graphite electrodes. LiDMP additive was synthesized using salt-solution mixing methods to study the electrochemical performance. During its preparation, an equal molar ratio of trimethyl phosphate and lithium iodide was added to 100.0 ml of acetone in an N_2-filled glove box. The final product was dried, collected, and used at 0.1 wt% during electrochemical testing. The surface film was formed by the LiDMP, which is the key to improving the charge transfer between the electrodes. It exhibits 91.5 % ICE which is higher than the cell without additive (87.9 %). The notable reason behind the remarkable performance and enhanced ionic conductivity are ascribed to the reduction of alkyl carbonates and the increase of $Li_xPO_yF_z$ compounds [51].

Post-mortem analysis of cycled LIBs, although carried out by very few researchers, reveals micrometer to nanometer-size structures. This also gives insights into the thickness of the electrode, the formation of SEI, and the chemical composition. For example, Aspern et al. explored three different phosphorous additives including tris(2,2,3,3,3-pentafluoropropyl) phosphate (5F-TPrP), tris(1,1,1,3,3,3-hexafluoropropan-2-yl) phosphate (HFiP), and tris(1,1,1,3,3,3-hexafluoropropan-2-yl) phosphite (THFPP). All of them were examined for their high voltage stability and flame-retardant capability. The NCM111/Li battery was operated in the 3.0–4.6 V range. The capacity retention with THFPP was 88.3 %, which is higher than other counterparts and standard electrolytes (56.3 %). The research showed that the electrode containing the 5F-TPrP surface was fully enclosed with decomposition products. Conversely, the 20.0 wt% 5F-TPrP additive enhances safety by reducing the electrolyte flammability more than others [52]. Further research is required to establish the electrochemical and thermal compatibility of NCM electrodes. All types of phosphate-based additives' capacity retentions are schematically drawn in Fig. 6, which shows the contribution of phosphate additives for LIBs.

The electrolyte additive should have the ability to control the HF attack in addition to cycle life and capacity retention increment. These properties are critical to safe battery operations. All previous phosphate additives have shown HF reduction after the interpretation of XPS results. However, recent studies depict that the Nuclear Magnetic Resonance (NMR) study is a very powerful tool to investigate HF content. For instance, Kim et al. used the NMR tool to quantify the HF content before and after bifunctional additive [53]. Analysis showed that 0.5 wt% of LiTSMP in the LNMO/graphite cell suppresses the HF formation. Also, these bifunctional additives are functional at high voltage and elevated temperature (45 °C) necessitating further research to develop safe next-generation batteries.

3.1. Flame retardant mechanism of phosphate additives

The phosphate flame retardant operates through the mechanism of scavenging free radicals [54]. In simple terms, the process involves heating and evaporating the phosphorus flame retardant. The resulting vapor generates P-containing free radicals, specifically phosphorous oxygen radicals (PO•). These PO· radicals effectively scavenge H• and HO•, which then terminates free radical reactions and inhibits flammability [55] as depicted in Fig. 7 (a). Researchers utilized theoretical simulations employing density functional theory, as depicted in Fig. 7 (b), to investigate the mechanism of free radicals. The simulations revealed a low binding energy between the flame-retardant molecules and harmful free radicals, indicating the flame-retardant's strong ability to capture them [56].

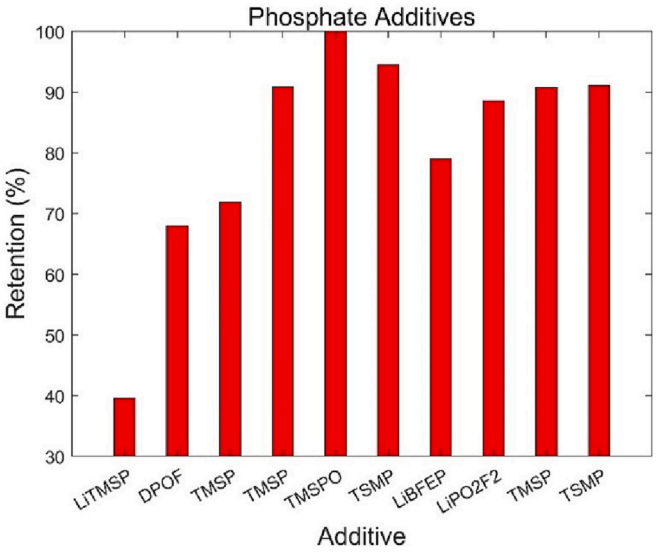

Fig. 6. Capacity vs. retention plots of phosphate additives.

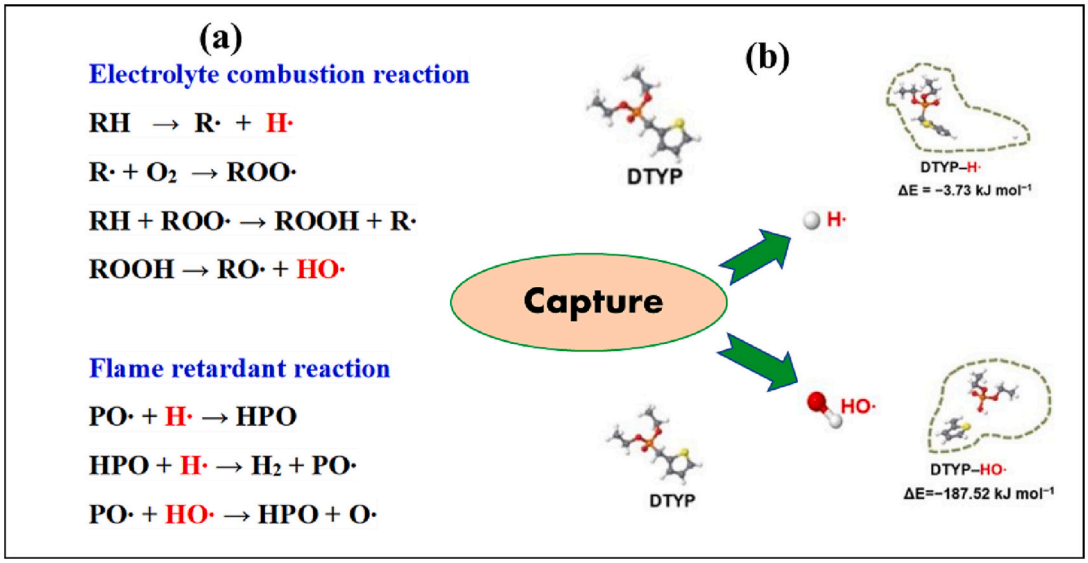

Fig. 7. Flame retardant mechanism for phosphate additives. Reproduced with the permission [55].

Phosphite additives are another class of chemicals that can be added to liquid electrolytes to improve LIB safety, alleviate thermal runaway, and improve electrochemical performance (see Fig. 8). Trimethyl phosphite (TMSPi) and trimethyl phosphate (TMSP) are added most to the $LiPF_6$ electrolyte to improve its performance. The working mechanism of the TSMPi+PCS is shown in Fig. 9. The oxidation state of phosphorus in TMSP(i) is three instead of five, which makes it thermally stable under high-temperature operations as well. Moreover, phosphite additives including tris(2,2,2-trifluoroethyl) phosphite (TTFP) have flame-retardant characteristics. Cycling tests of the TTFP electrolyte conducted in the form of a 2032-coin cell at a discharge rate of 1C in the 2.75 V–4.20 V range at 40 °C showed better discharge and retention capacity. The cell with the DPOF additive showed better cyclability. The performance was found to be better at 40 °C compared to the room temperature [57].

The thermal stability of LIBs is critical to their operations when used under harsh environmental conditions and in machines that require elevated power to operate. Their application in mining machinery including loaders and haul trucks is one such example. However, cathode capacity is reduced when operating at high voltages or high temperatures. Phosphite additives can increase the efficiency working temperature range of the electrolytes. Research has shown that the addition of 0.5 wt% tris(trimethylsilyl) phosphite (TMSPi) to the conventional $LiPF_6$ electrolyte impedes the serious oxidation of the electrolyte, usually observed at 4.8 V. Instead, the additive-laden electrolyte decomposes at 5.1 V. The stability of the SEI is also improved. The capacity retention of the electrolyte improved to 91.2 % after 100 cycles. The charged cell was also observed to maintain its voltage after 15 days with the additive [58]. The TMSPi additive added to the electrolyte lowered the cell impedance significantly. Adding vinylene carbonate to graphite cells containing TMSP decreased the parasitic reactions [39]. Tris(2,2,2-triflouroethyl) phosphite electrolyte additive leads to film formation on the electrode surface that enhances the battery performance. This was shown to be an electrolyte flame-retardant as an additive at 15.0 wt%. It enhances the CE of the lithiation and de-lithiation cycle [59]. Experiments with TMSPi and TMSP added to 0.2 g 1.0 M $LiPF_6$ electrolyte showed diminished flammability. White smoke of P_2O_5 was observed, which is an efficient flame retardant, especially in the TMSPi additive [60]. This additive encourages the formation of an oxide and phosphorous (P_xO_y-type) rich relatively thick film on the positive electrode during cycling. This impedes the increase in cell resistance, lowers the dissolution of metal oxides, and retains the cell capacity [61]. The addition of TMSP to the electrolyte inhibits the cathode structural breakdown due to uniform film growth during cycling. TMSPi lowers electrolyte decomposition even at high voltages and alleviates HF formation. Its addition also enhances discharge capacity retention from 55.9 % to 77.1 % [62]. TMSPi stabilizes the oxygen species on the cathode which leads to an augmentation in the cycling performance of lithium and graphite half cells. The thermal stability of the electrode and the electrolyte is also improved with its addition as shown by a rise in decomposition temperature.

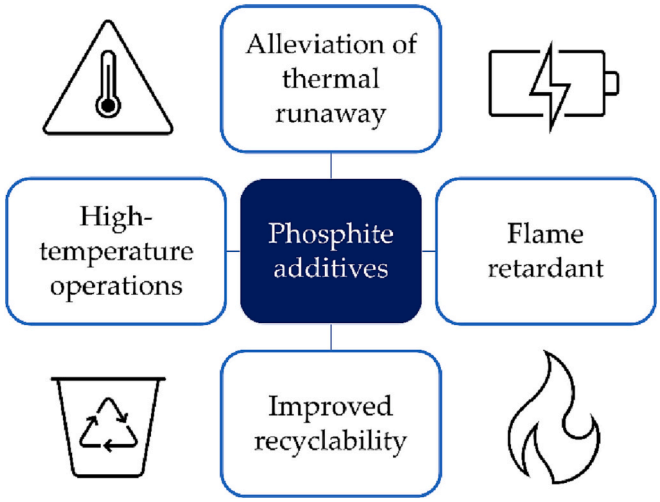

Fig. 8. Advantages of phosphite additives.

The phosphite additives improve the discharge capacity of LIBs. For example, it is improved to 280.0 $mAhg^{-1}$ in the second cycle and 230.0 $mAhg^{-1}$ after 110 cycles for a cell with a lithium-rich layered oxide cathode. The additive also improves the charge retention of the cell which is another indicator of a better discharge capacity [63]. Stabilization of the electrode is also observed with the addition of triphenyl phosphite. The cycling performance of high-voltage lithium-ion batteries using $Li_{1.16}Ni_{0.2}Co_{0.1}Mn_{0.54}O_2$ as cathode materials is also improved. This is due to the protective film formation on the phosphite added to the electrolyte. Polarization of the electrode decreases at higher temperatures which enhances the battery-specific capacity. All the performance improvements are observed when the additive

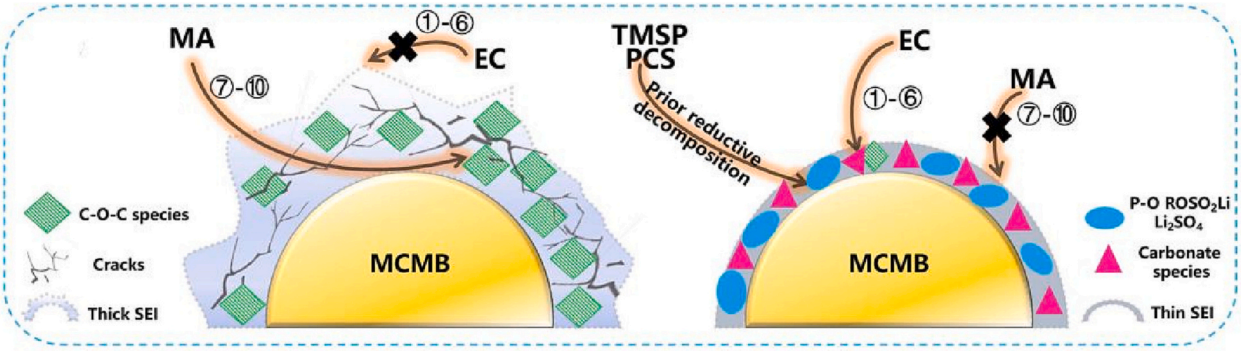

Fig. 9. Working machanisim of TSMPi + PCS.
Reproduced with permission copyright (2019) Elsevier [68].

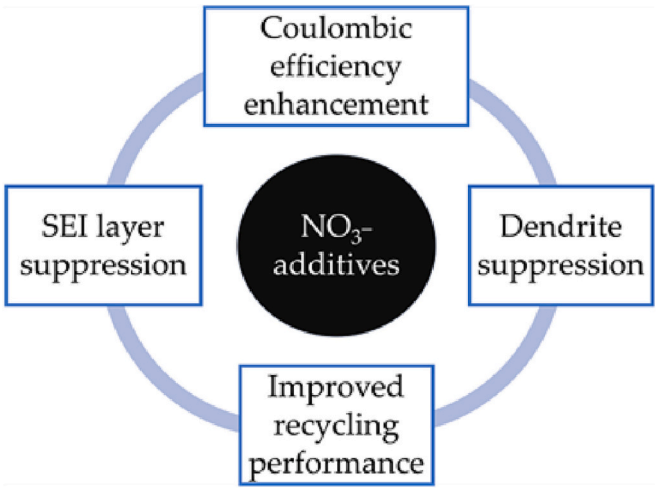

Fig. 10. Advantages of nitrate additives.

concentration is low. A 1.0 wt% added additive lowers the discharge capacity of the battery to about 140.0 $mAhg^{-1}$ [64].

Phosphite additives have been shown to lower the generation of harmful byproducts during the operations cycle. For example, the TMSPi additive is effective in lowering the HF gas concentration. This highly reactive byproduct is generated due to the presence of impurities in the electrolytes. HF reacts rapidly with the cathode, and electrode degradation is enhanced significantly beyond the 5.0 V operation. This is shown by fundamental calculations on reaction pathways for tris(trimethylsilyl) phosphite, $P(OSi(CH_3)_3)_3$ additive in electrolytes [65]. The additive, however, reacts with $LiPF_6$ electrolyte at room temperature leading to aging. The fluorophosphate generated during the reaction inhibits the formation of the SEI layer but leads to deterioration of the cycling stability ability at about four weeks. This indicates that the phosphite additive is most effective when fresh [66]. Although the addition of triethyl phosphite and tris(2,2,2-trifluoroethyl) phosphite were both shown to lead to the formation of a protective coating and have a lower oxidation potential compared to the electrolyte, lithium-ion mobility through the interphase layer is lower for the triethyl phosphite additive. The tris(2,2,2-trifluoroethyl) phosphite additive, therefore, leads to better CE and capacity retention [67]. Very recently, ester carbonate additives played a very important role in enhancing the battery performance in the range of −60 °C to 50 °C [68].

Numerical modeling tools including density functional theory (DFT) have supported the performance of phosphite additives in batteries. Kohn-Sham calculations were used to evaluate various electrochemical properties that were later validated with experiments. The computer models indicated that 17 phosphite molecules may undergo reactions at the anode. TMSPi removes the unwanted HF molecules from the electrolytes and improves cell performance [69]. Studies have also shown that these additives can remove HF and LiF species from the electrolyte and the cathode [70]. Further, DFT calculations were used to develop screening protocols based on Gibbs free-energy calculations to select suitable additives for high-voltage lithium-ion batteries. Phosphite additives including trioleyl phosphite, tris(1-adamantyl) phosphite, distearyl pentaerythritol diphosphite, and tritertbutyl phosphite were recommended as suitable additives [71]. Experimentally validated chemical and DFT computations have also helped in the understanding of parasitic oxidation currents at high voltages that lead to the lowering of battery impedance in the presence of additives. DFT simulations result explained the mechanism for cathode protection after adding the

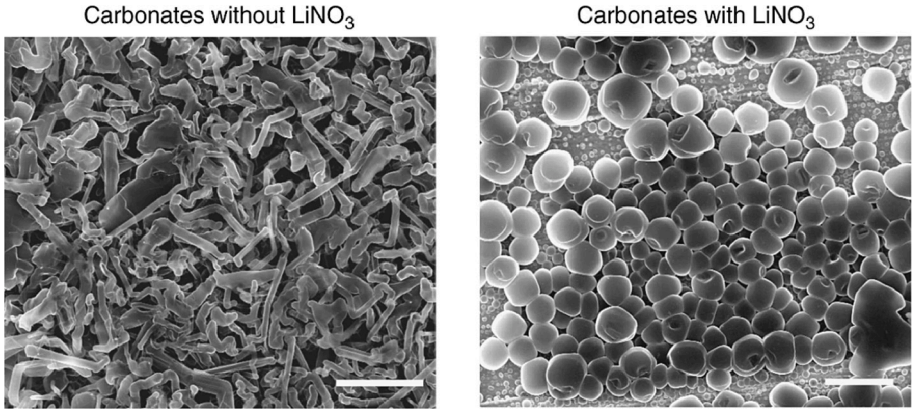

Fig. 11. SEM images with and without Nitrate based additives.
Reproduced with permission copyright (2018) Nature Communications [75].

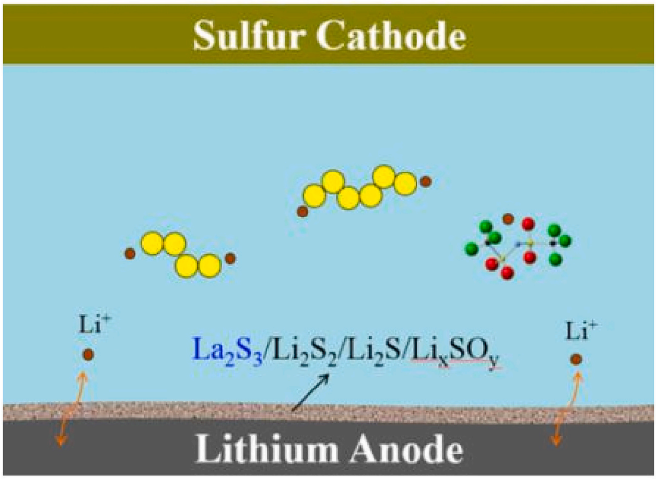

Fig. 12. Scheme for passive composite film formation on the Li-anode by adding $La(NO_3)_3$.
Reproduced with permission Copyright © 2016, American Chemical Society [88].

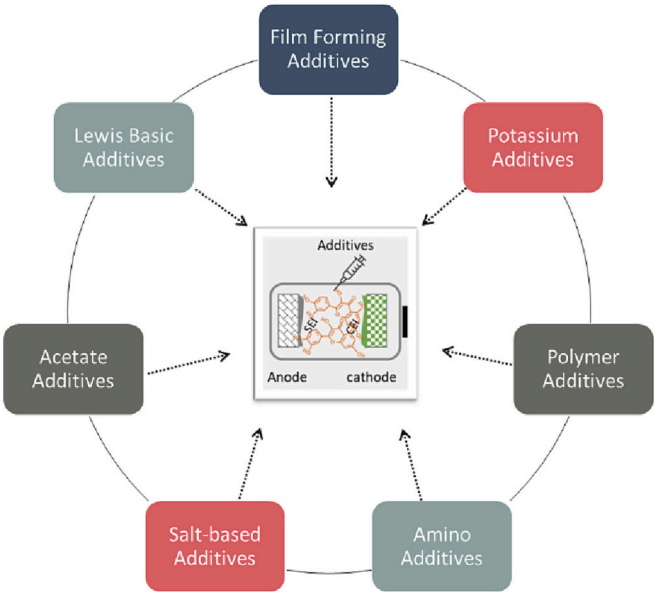

Fig. 13. Other additives for Li-ion battery applications.

phosphite additives. The PF_2OSiMe_3 product is formed when the tris (trimethylsilyl) phosphite undergoes a reaction with $LiPF_6$ resulting in delay to the parasitic oxidation of the solvent. This stabilizes the interfacial resistance [72] which is critical to safe LIBs.

3.2. *Flame retardant mechanism of phosphite additives*

Phosphites exhibit distinct characteristics compared to other phosphorus-containing additives. With an oxidation number of three (P (III)), the phosphorus center atom carries a pair of lone-pair electrons. While both phosphate and phosphite flame retardants enhance thermal stability significantly, phosphite additives outperform phosphates due to the lower oxidation state of phosphorus in the compound. When introducing a phosphite additive, such as trimethyl phosphite, to the $LiPF_6$-based electrolyte, it undergoes combustion, resulting in the formation of P_2O_5 (solid) as a result of P(III). This solid flame retardant plays a vital role in reducing the potential for battery fires [60]. Furthermore, the inclusion of a fluorinated substituent, like a PF_5 stabilizer, allows for an effective combination with PF5 derived from the decomposition of $LiPF_6$. This combination effectively suppresses the reactivity and side reactions of PF_5 while enhancing the stability of $LiPF_6$ [73].

4. Nitrate additives

Nitrate-based additives are attractive alternatives to the contemporary carbonate-based additives used in LIBs. The incorporation of nitrate additives leads to several benefits including CE improvement, suppression of SEI layer and dendrite formation, and enhancement of recycling characteristics (see Fig. 10). The addition of nitrate additives to electrolytes has shown a significant improvement in battery performance. This is attributed to several mechanisms including the promotion of Li^+ ion dissolution that predominantly happens via the cation transfer to the solvation shell and alteration of their surroundings [74].

Nitrate additives result in CE enhancement which is a strong indicator of superior battery performance. This occurs due to the rapid reduction of NO_3^- ions that impact the lithium deposition morphology. Cations also impact additive performance significantly. For example, experiments showed that the KNO_3 additive performed at par or better than Li, Na, and Cs when their CE values were compared [75]. Moreover, the cells that used Na and Cs-based electrolytes began to show unstable CE values after 60 cycles. Since the abundance of K elements in the earth's crust is much higher (approximately ×380) than the Li element, using K-based electrolytes is more favorable economically [76]. Frequent, repeated cycles of operations lead to the lowering of the CE of the battery even in the presence of nitrate additives including $LiNO_3$. A new electrolyte system with an elevated $LiNO_3$ concentration was developed that exhibits a CE exceeding 99.0 % for greater than 200 cycles compared to 35 cycles with conventional $LiNO_3$ electrolytes [77].

Dendrite formation is a major drawback of LIBs that leads to undesirable internal currents. Dendrites are formed due to uneven nucleation and metal crystallization process. They are impacted by current density and temperature and could have a deposition height of 10.0–200.0 μm [78]. Dendrites significantly lower the CE values of the battery [75]. Nitrate additives, for example, potassium nitrate, have been shown to effectively suppress their formation [79]. Primarily, electrolytic shielding due to the K^+ in the additive impedes the dendrite formation [80]. The K^+ ions with a higher redox potential are drawn towards the lithium dendrites by electrostatic attraction while the NO_3^- is reduced and strengthens the SEI. The nitrate additives alleviate the formation of the SEI layer, depending on the electrolyte characteristics, on the lithium metal anode (LMA). Several nitrate additives lead to multi-facet improvements in battery performance. For example, Potassium Nitrate (KNO_3) was recently demonstrated to improve the electrochemical performance in addition to suppressing the K^+ dendrite growth effects [80]. Addition of nitrate additive results in the formation of spherical Li nuclei during deposition instead of dendrite shaped as visible in Fig. 11.

Nitrate additives also improve the cycling characteristics of the battery. The lithium nitrate additive lowered the Li anode's low hysteresis behavior for 1000 h at a current density of 0.5 mA. Experiments in the presence of $LiNO_3$ showed a significantly cleaner electrode surface after cycling which could be attributed to a change in the growth mechanism of lithium nanoparticles. Further research using a Li-graphite dual-ion battery also showed similar excellent cycling capabilities. The battery was observed to retain about 97.0 % of its storage capacity and operated at 95.0 % CE after 300 cycles [81]. Additionally, the insoluble Li_2O generated during the reaction of $LiNO_3$ additive with the Li metal results in the development of a protective SEI on the Li metal. This protective layer inhibits rapid oxidation of the electrode. Subsequent chemical reactions that involve LiO_2 produced during the oxidation phase led to the generation of $LiNO_3$ in the presence of dissolved oxygen. This also explains the cycling of $LiNO_3$ additives in the batteries [82]. Solid electrolyte interface layers are critical components of rechargeable LIBs and are formed whenever lithium ions contact salts and solvents. This layer slows down the corrosion of the lithium surface

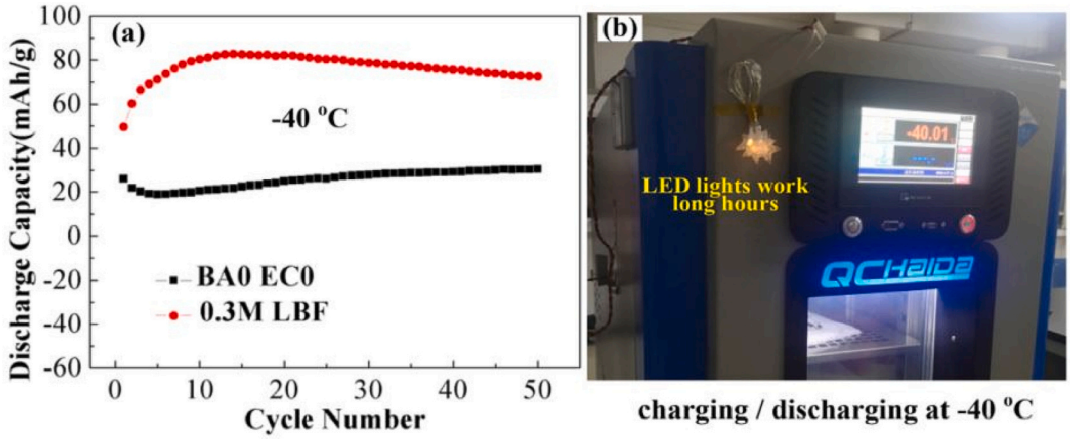

Fig. 14. Cycling performance with different electrolytes.
Reproduced with permission copyright (2021) Elsevier [106].

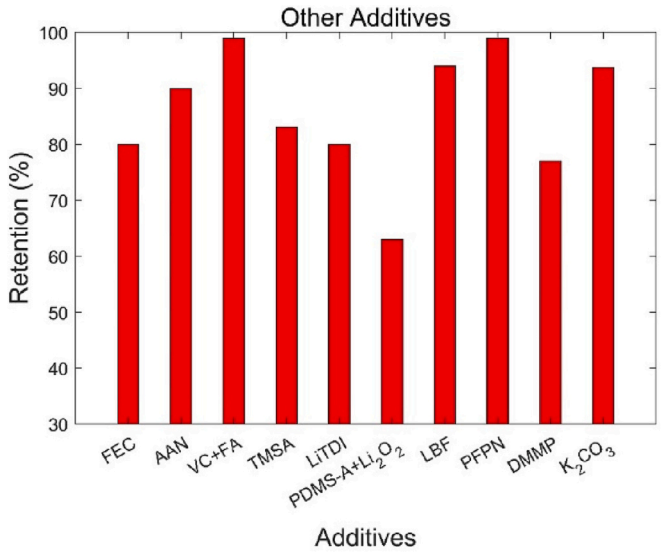

Fig. 15. Capacity vs. retention chat for other additives.

and plays an indispensable role in LIB safety, shelf-life, and capacity. These layers are formed on the anode during the initial cycle of operations when the electrolyte solvent compounds and the salts decompose, but their formation mechanism is still not well understood [83,84]. Some of the major components of the SEI layers include $(CH_2OCO_2Li)_2$, Li_2CO_3, polycarbonates, $Li_2C_2O_4$, and several others [85–87].

An example of a suitable electrolyte additive for stabilizing the lithium electrode surface is lanthanum nitrate. This additive facilitates the formation of a passivation film on metallic lithium, as depicted in Fig. 12. The passivation film may consist of lanthanum/lithium sulfides. Essentially, when $La(NO_3)_3$ is introduced into the electrolyte, La^{3+} quickly undergoes reduction by Li, leading to the formation of metallic La. Subsequently, metallic 'La' reacts with polysulfide anions to produce La_2S_3 on the surface of Li. Along with the deposition of Li_2S_2/Li_2S and Li_xSO_y, this composite passivation film forms on the Li anode, which helps reduce the reducibility of metallic lithium and minimize electrochemical deposition on the anode. Ultimately, the stabilized passivation film, approximately 24 μm thick, contributes to enhancing the cycling and ionic conductivity of the Li—S cell [88].

Since the $LiNO_3$ additive in the electrolyte is consumed continuously during the chemical reaction, the battery performance depends on its concentration. Several researchers have also explored the cyclability of the batteries in the 0.0–1.0 M concentration range. The cells with 0.5 M and higher $LiNO_3$ concentration show cycling efficiency exceeding 95.0 %. A LiCu cell showed CE lower than 90.0 % when the $LiNO_3$ concentration was less than 0.25 M [89]. Recently, there has been an increased interest in rare earth elements. Research has shown that concentrated (0.05 M) rare earth nitrates can be dissolved in commercial carbonate electrolytes. Quantum chemistry calculations and molecular dynamics simulations on yttrium nitrate $Y(NO_3)_3$ additive added to the conventional $LiPF_6$ electrolyte showed that the solvation structure of Li^+ could be altered due to fluoroethylene carbonates (FEC) and rare earth ions [90]. The nitrate additives, therefore, can significantly improve the performance of LIBs.

Despite several benefits, nitrate additives usually have low solubilities in traditional carbonate-based electrolytes. This could sometimes lead to a low CE and limit its application in LIBs. Research using an 18-crown-6 coordinated ether showed the promotion of the dissociation of the $RbNO_3$ additive. The NO_3^- ions are released and lead to a marked improvement in Li^+ deposition. The $Rb(18\text{-crown})^+$ formed during the process suppresses the formation of irregularly shaped dendrites that lower the cell efficiency and could lead to short-circuiting and other problems. This also provides for a pathway to stabilize an LMA in a conventional carbonate-based electrolyte [91]. Other plausible methods include filling the separator with solid $LiNO_3$ powder or introducing them using carrier salts. The addition of up to 10.0 wt% of $LiNO_3$ and fluoroethylene carbonate (FEC) additives modifies the solvation structure of the commercial carbonate electrolytes. This increases the lithium CE up to 99.6 % in 100 cycles and retention of up to 90.8 % after 150 cycles promoting practical applications of high energy density batteries [92].

4.1. Guidance for the development of new nitrate additives

When it comes to stabilizing the solid electrolyte interphase (SEI) layer, nitrate additives have garnered significant attention in the literature. While their usage is primarily observed in Li-metal batteries like Li—S, it is important to note that nitrate additives offer notable benefits for improving the overall performance of such batteries, particularly when used in conjunction with FEC additives. By utilizing nitrate additives, the SEI layer of Li-metal batteries can be effectively stabilized. This is crucial because a stable SEI layer is essential for reducing the reactivity between the lithium metal anode and the electrolyte, thereby enhancing the battery's overall performance and lifespan. Furthermore, the nitrate additives exhibit a remarkable CE for Li plating and stripping processes, ensuring efficient charge and discharge cycles.

5. Other additives

In this section, the synthesis, evaluation, and execution of other additives which have not been discussed in the previous sections are reviewed critically. This also provides a path to research these additives. Many of these are not synthesized and used in the LIB technology currently, but show remarkable performance, including thermal stability and promising electrochemical properties at room and elevated temperatures. According to their main components, these additives are classified and laid out in the schematic diagram shown below (Fig. 13).

Film-forming additives may create an extra layer that helps to protect the surface of electrodes. Their main purpose is to create an artificial passivation layer on the surface of the electrode. Hence, the additives must be selected to meet the basic requirement of physicochemical properties. Very few species mentioned in Sections 2–4 are used as film-forming additives. Among them, organic additives are extensively studied for their film-forming capability and stability during electrochemical reactions. In the past, additives such as fluoroethylene carbonate (FEC), vinylene carbonate (VC), and ethylene sulfite (ES) were proposed, all are very favorable to making graphite anodes. For example, R. Mogi et al. used three additives along with the 1.0 M $LiClO_4$ in PC and investigated the film formation using AFM techniques [93]. Using an experiment, they confirmed that 5.0 wt% of FEC additive was formed homogeneously on the surface. The estimated particle sizes are 100.0–150.0 nm in diameter. In comparison, other additives have no uniform surface coverage and show high resistance that hinders the battery's performance. Afterward, butylene sulfite (BS) was synthesized and used as a film-forming additive and tested for its thermal stability using the DSC analytical tool. The DSC results show exothermic peaks between −100 °C and 180 °C that indicates that the BS additive has high stability at low temperatures. Their remarkable performance could be attributed to, (i) the lowest unoccupied molecular orbital (LUMO) energy and the total energy of the carbonate molecules being higher than that of sulfite molecules, (ii) the formation of ion pairings, and (iii) the growth of lithium-oxy-sulfite film (Li_2SO_3 and $ROSO_2Li$) [94]. These additives were not explored in terms of long cycling life at high temperatures or any storage condition to prove the thermal stability. Still, this research extended to various types of additives which will be described in this section to discuss their unique contribution to safe LIBs.

Acid-based electrolytes promote good LIBs performance in the 100–1000 cycles range. Acrylic acid nitrile (AAN) is one such film-forming organic additive. AAN reduction and electrochemical polymerization of the vinyl group is the lead reaction for the SEI formation in which electropolymerization plays a crucial role [95]. Very long-term cycle life (over 1000 cycles) and high energy density of materials are prerequisites to meet the current energy scenario. However, the studies investigated the performance only for 15 cycles, which is not a good indication of the long-term cycling of the LIBs. Also, it has been reported that vinylene carbonate (VC), an organic additive, contributes to the radical polymerization process which leads to the growth of passivation film [96]. Even at 60 °C, the VC-containing electrolyte shows functionality such as ionic conductivity which was validated by XPS analysis. The film-forming 1-fluoro propane-2-one (FA) additive was investigated by Kramer et al. [97], who suggested that FA additive (1.0 wt%) along with 1.0 M $LiPF_6$ in PC with 1.0 % VC exhibits an ICE of 75.0 %. Also, it provides a discharge capacity of 360 mAh g^{-1} with a capacity retention of more than 99.0 % after 100 cycles. This cycle life is higher than previously reported film-forming additives. This acid-based additive can be effectively used to suppress graphite exfoliation by PC co-intercalation. Also, FA creates constructive SEI in PC solvent specifically mixed with VC additive.

Organic electrolytes are efficient during tests at higher rates up to 3C. Various organic compounds have been introduced as an additive to protect electrodes against overcharging issues of LIBs. Watanabe et al. proposed different organic additives with heteroatoms such as nitrogen, oxygen, fluorine, silica, phosphorous, and sulfur for 4.0 V cells. Among them, the trimethyl-3,5-xylyl silane additive acts as an overcharge shield due to its potential E_{ox} (around 4.7 V). Also, this additive is stable up to 60 °C due to the potential difference ($E_{ox} = 0.07$ V) [98]. A new organic antioxidant additive called quercetin was shown to enhance cycle life, battery safety, and overcharging tolerance. In this study, a $LiCoO_2$/graphite prismatic soft pack cells system with a 0.05 % quercetin additive was selected. The tests showed that the discharge capacity was 1196.0 mAh/g at a current density of 550.0 mA without the additive. With the quercetin additive, the discharge capacity was 1177.0 mAh/g [99]. These findings suggest that the electrolyte additive did not alter the electrochemical properties but held capacity stability during high current delivery usages. Additionally, Lewis basic additives are also researched due to their thermal stability. They can be of either hexamethoxy-cyclotriphosphazene (HMOPA) pyridine or hexamethylphosphoramide (HMPA) forms. They were studied with the $LiPF_6$ in EC/DMC/DEC mixed by weight 1:1:1. They, in low concentrations (3.0–12.0 wt%), were shown to enhance thermal stability. For this research, $LiNi_{0.8}Co_{0.2}O_2$ was selected as a cathode and mesocarbon microbead (MCMB) as an anode. Storage tests at 80 °C showed that higher concentrations of HMOPA can be used for flame suppression. This research finding highlighted that HMPOA added additive secured the electrode from dangerous by-products such as PF_5 and LiF [100].

Apart from organic additives, novel acetate and ionic liquid-based electrolyte additives can provide a high capacity between 150 and 1200 cycles. For example, trimethylsilyl (trimethyl siloxy) acetate (bis-TMSA) additives help to enhance physical and electrochemical results. In one study, high-voltage cathode materials were examined for film formation after cycling with and without additives. Electrochemically, the additive provided initial charge and discharge capacities of 338.41 mAh g^{-1} and 237.56 mAh g^{-1}, respectively [101]. Remarkably, excellent cyclability and rate capability were observed after using 1.0 wt% bis-TMSA-containing electrolyte. This finding suggested that the acetate additive contributes to enhancing battery safety by suppressing the fluorine formation on the surface of the electrode. Similarly, electrolyte (ionic liquid) salt introduced as an additive for silicon-based electrolytes has shown several improvements in LIB performance, especially in higher capacity retention. The most recent electrolyte salt utilized with silicon anode is lithium 4,5-dicyano-2-(trifluoromethyl) imidazolide (LiTDI). Lindgren et al. investigated LiTDI electrolyte salt along with film-forming additives like FEC and VC. Cycling performance and SEI formation of Si electrodes were investigated using a cycler and XPS. Both studies' results were compared with LiTDI + FEC + VC additive and pure LiTDI. The research without additives showed that the SEI is smooth and primarily composed of lithium alkyl carbonate solvents with a low LiF content [102]. In general, the additives favor an SEI with high proportions of LiF and a large extent of polycarbonate species.

The SEI and LiF are advantageous to the cycling performance of composite Si electrodes. Research on the LiTDI additive amount optimization to control the SEI thickness and performance enhancement was carried out by Xu et al. [103]. Xu's research group examined the moisture-scavenging electrolyte additive which can adequately restrain the hydrolysis of $LiPF_6$. The storage study reveals that no $LiPF_6$ degradation was found after storage for 35 days with 2.0 wt% LiTDI. It improved the electrochemical performance and thermal stability of the battery. The moisture-scavenging mechanism had been demonstrated by operating the NMC/Li cells at 55 °C for 1000 cycles. DFT studies using the Gaussian G09 package validated this result. Some organic additives are stable at high temperature (55 °C–70 °C) regions and in the −20 °C to −40 °C range at low temperatures.

5.1. Guidance for development of new Imidazolide additives

The formation of the SEI/CEI on the electrode surface is crucial for the proper functioning of rechargeable LIBs, especially those utilizing Imidazolide as electrolyte additives. It is essential to select a bifunctional or multifunctional imidazole that can concurrently form a protective

film, reduce polarization, and stabilize the interface layers. These interface layers contribute to the stability of the electrolyte/electrode interface, effectively mitigating solvent decomposition and protecting electrode materials from corrosion during the charge and discharge processes. As a result, the performance of batteries can be greatly improved. Such bifunctional additives have the potential to advance the development of next-generation LIBs. Additionally, several factors must be considered before using any imidazole-based liquid additives, such as suppressing the severe oxidative decomposition of carbonate solvents and the salt, as well as reducing the dissolution of metal ions like Mn, Co, and Ni. When considering the SEI formation with imidazole additives, it is important to consider the binding energies of the embedded particles. These measures will facilitate the migration of Li^+.

The synergistic effects of various organic additives were also studied to understand atomic-level changes and how the additive impacts electrode performance. Zhu et al. evaluated the synergistic effect of various functional electrolyte additives such as $LiB(C_2O_4)_2$, ($LiF_2B(C_2O_4)$, triphenylamine, and 1,4-benzodiozane-6,7 diol [104]. In this study, they used different cathode compositions and a graphite anode. During the cycling, they found that $LiB(C_2O_4)_2$ is a good additive for diminishing battery capacity loss. However, all additives exhibit better performance at 30 °C and 55 °C when compared to the standard electrolyte. Still, further studies are required to reveal the SEI due to the incomplete test conditions. Recent research showed potassium ions (K^+) intercalated graphite and carbonate ion CO_3^{2-} on graphite improve LIBs performance due to the formation of CH_3 radicals. Potassium carbonate has also been used as a film-forming additive for LIBs. The addition of K_2CO_3 effectively conceals the reduction of EC during the initial lithiation. The formation of SEI was measured by Zhauang et al. using EIS at different discharge potentials starting from 2.0 V–3.0 V. Finally, they proposed that this additive can hold up the resistance of SEI film and viscoelasticity of SEI film [105].

Solvents in the LIB electrolyte must have high solubility, high conductivity, and low viscosity. Commercial solvents like EC/EMC and PC etc. meet those requirements despite having some drawbacks that hinder the LIB's real application. For instance, low dielectric constant leads to low solubility and dissociation of electrolyte salt. To address these drawbacks, Lv et al. worked on solvent and lithium salt to enhance the low-temperature performance. In this study, they used BA + EC + LBF mixed additives to improve the performance. The battery showed 119.3 mAh/g capacity with additives, whereas without additives it showed only 74.3 mA/g capacity at −40 °C shown in Fig. 14 (a) and (b) representing good stability [106]. It could be ascribed that the formation of thin LiF at the cathode electrolyte interface helped to boost the Li-ion diffusion.

Novel polymer additives maintain high stability between −20 °C–70 °C. Emerging polymer-based liquid additives exhibit excellent low-temperature performance. For example, Kim et al. studied different polymers' and copolymers' electrochemical properties at low temperatures (−20 °C) with electrolytes such as polydimethylsiloxane (PDMS), poly[dimethylsiloxane-*co*-(siloxane-g-acrylate)] (PDMS-A), poly(dimethylsiloxane-*co*-phenyl siloxane) (PDMS-P), and poly [dimethylsiloxane-*co*-(siloxane-g-ethylene oxide)] (PDMS-EO). From this analysis, they discovered that PDMS (A) shows high-rate capability at low temperatures while PDMS-P shields the EC and DMC parts from freezing at −20 °C [107]. These findings suggest that the polymer contains grafted functional groups which help in improving performance at extreme temperatures. Further research is required to understand more about both electrodes. Later, the same research group used PDMS-A and Li-modified silica nano salt (Li_2O_2) and studied the low-temperature performance at −20 °C. This battery operated with 1.0 wt% of PDMS-A and Li_2O_2 and was evaluated in the −20 °C to −70 °C range. The cycle performance is excellent at room temperature and −20 °C due to the availability of the functional groups in both additives. The capacity retention of Li_2O_2-added additives was 60.9 % after 50 cycles while PDMS-A had only 53.3 % [108]. Even though some low-temperature tests were done, detailed electrochemical relationships still need to be explored. These should address the synergistic effect quantitatively and qualitatively.

Recently, alkyl phosphates have been probed due to their non-flammability properties. Phosphoric acid ester amide is a new class of self-extinguishing solvent that has been studied as an electrolyte additive. For example, Shiga et al. used amide additives to investigate the self-extinguishing properties and thermal stability of batteries [109]. In this research, dimethylamino-di(trifluoroethyl) phosphate (PNMeMe) and methyl phenylamino-di (trifluoroethyl) phosphate (PNMePh) phosphoric acid amides were used. Overall, the PNMePh showcases good thermal stability compared to the fluorinated phosphate. Even if the reductive voltage of PNMePh was 0.61 V vs. Li^+/Li, it was reduced by an extremely strong solution of PNMePh. This research provides a new direction for using multifunctional electrolyte additives that will impact future safe Li-ion batteries. The other additives vs. capacity retentions are compared in Fig. 15, which are collected from the literature, and the data represents both room, high, and low temperatures.

6. Development of new electrolyte additives and their selection criteria

Due to the large number of electrolyte additives that can be used to enhance the performance and safety of LIBs, the selection of the most suitable additive for a specific application is difficult. Usually, these additives are chosen for their general safety, enhancement of electrode properties, stability of salts, overcharge protection, flame retarding properties, and improvement of the SEI layer performance [110]. However, there are many specific tools, criteria, and methodologies that can be used to select, and in certain cases to develop, efficient additives. The functionality selection principle is one of the most commonly adopted means to select the most suitable ones [111–113]. In this process, useful functionalities of different additives are incorporated into one molecule to make them more efficient for a particular application. For example, cyclic fluorinated phosphates were designed to stabilize the surface of MNC532 cathode [111].

Accurate numerical modeling techniques including density functional theory (DFT) models are applied to develop and select the additives. Several additives have been developed using fundamental principles of molecular dynamics to predict their performance. For example, 1,3-dimethyl-2-imidazolidinone (DMI) additive's performance was evaluated with and without vinylene carbonate using DFT calculations and experiments that showed good agreement [114]. Recently, 1,1-(5,14-dioxo-4,6,13,15-tetraazaoctadecane-1,18-diyl) bis(3-(sec-butyl)-1H-imidazol-3-ium) bis((trifluoromethyl)-sulfonyl) imide additive was synthesized that enhances the LIB life, showed better cycling performance, and better discharge capacities [115]. Gaussian 09 package was used for DFT computations. The effect of fluoroethylene carbonate (FEC), when added to the silicon anode of a LIB, was studied through DFT calculations and validated experimentally. This research showed a four-fold lowering of the cell impedance [116].

Other additives that were developed based on DFT calculations include boron-nitrogen-oxygen alkyl group called methylboronic acid ester, vinyl ethylene carbonate (5.0 vol%), malonic acid-decorated fullerene, 4-(Trifluoromethyl)-benzonitrile, sulfur-containing compounds like 1,3-propane sultone, lithium difluorophosphate, lithium 4-benzonitrile trimethyl borate, and several others [117–121,50]. The type, number, and position of the functional group in an additive is critical for their efficacy and is another parameter that allows their specific applications. For example, 1,3,2-dioxathiolane-2,2-dioxide (DTD) is considered an efficient additive for its ability to use its five-member rings during the electrochemical reaction [122–124]. The additive, 4-(trimethylsiloxy)-3-pentene-2-one has siloxane and carbon-carbon groups that allow the lowering of HF generation and higher CE [125]. Additives like zwitterionic compounds with ester and sulfonate groups, organosilicons with octamethylcyclotetrasiloxane and

octamethylcyclotetrasiloxane, isocynate compounds, and lithium alkyltrimethyl and aryl-trimethyl borates have been developed that improve the LIB performance [126–130].

Data sciences, machine learning, and artificial intelligence-based methodologies are being used for the prediction of battery performance and the appropriate battery component materials including the electrolyte additives [131–136]. The Electrolyte Genome Project uses big data to calculate molecular properties of battery materials [137]. The Bayesian optimization technique was used recently using open circuit voltage gradient and CE to optimize the concentrations of fluoroethylene carbonate and vinylene carbonate for an NMC-622/graphite LIB in a pouch configuration [138]. The impacts of vinylene carbonate, lithium bis(oxalate) borate, and fluoroethylene carbonate additives were studied on an NMC622/graphite cell using artificial neural network models. The models predicted a capacity of 160 mAhg-1 and a retention of 65.0 % after 100 cycles [139].

7. Conclusion and prospects

The liquid electrolyte system plays a crucial role in ensuring the safety of batteries, which requires a deeper understanding of its core materials and more advanced analytical tools for in-depth visualization. Although additive-based liquid electrolytes have made significant progress in enhancing the safety performance of LIBs, the issues have not been completely resolved. Therefore, we suggest several conceivable directions for next-generation safe Li-ion research. Some of them are shown below:

(i) The rapid increment in temperature inside the battery cell leads to thermal runaway, which can be addressed by using advanced characterization tools to measure the internal battery conditions after introducing electrolyte additives. In-situ Raman spectroscopy can reveal the concentrations of ions at different positions in the electrolyte solution. Earlier troubleshooting will help avoid the risk of a big battery fire.

(ii) More research on additive-based liquid electrolytes is required with LIB sizes and storage ratings ever increasing. Thematic areas that could be explored include enhancing their cycle lives for practical applications such as electric vehicles.

(iii) Both high and low-temperature conditions are critical, leading to battery fire risks. Several electrolyte additives have been studied in the high-temperature region, but few studies are available for low-temperature conditions. Therefore, more research is recommended on their performance in low temperatures (e.g., −20 °C to −70 °C).

(iv) Computational prediction is essential to ensure the synergistic properties of electrolyte additives, such as electronic structure, defect, and Li trapping. Using DFT simulations, the feasibility of new formulations with different elements can be predicted, particularly for electrolyte additives containing Li-salt.

(v) Exploring new materials is another way to find suitable electrolytes for safe Li-ion batteries. For instance, ionic liquids can build a robust interface between electrode materials, exhibit non-flammability, boost ionic conductivity, and increase coulombic efficiency. Finally, studying the relationship between thermal and electrochemical properties is crucial for implementing large-scale safe batteries in modern-day applications that require high power.

Declaration of competing interest

There are no conflicts to declare.

Data availability

No data was used for the research described in the article.

Acknowledgments

This research is funded by the National Institute for Occupational Safety and Health (NIOSH) under contract number 75D30120CO8913 and 1 U60OH012350-01-00. The findings and conclusions in this paper are those of the authors and do not represent the official position of the National Institute for Occupational Safety and Health, Centers for Disease Control and Prevention; nor does mention of trade names, commercial practices, or organizations imply endorsement by the U.S. Government.

References

[1] T. Kim, W. Song, D.Y. Son, L.K. Ono, Y. Qi, J. Mater. Chem. A 7 (2019) 2942–2964.
[2] A. Masias, J. Marcicki, W.A. Paxton, ACS Energy Lett. 6 (2021) 621–630.
[3] A. Mishra, A. Mehta, S. Basu, S.J. Malode, N.P. Shetti, S.S. Shukla, M. N. Nadagouda, T.M. Aminabhavi, Mater. Sci. Energy Technol. 1 (2018) 182–187.
[4] Z. Liu, Y. Jiang, Q. Hu, S. Guo, L. Yu, Q. Li, Q. Liu, X. Hu, Energy Environ. Mater. 4 (2021) 336–362.
[5] D. Aurbach, Y. Talyosef, B. Markovsky, E. Markevich, E. Zinigrad, L. Asraf, J. S. Gnanaraj, H.J. Kim, Electrochim. Acta 50 (2004) 247–254.
[6] K. Xu, Chem. Rev. 114 (2014) 11503–11618.
[7] N. Chen, Y. Dai, Y. Xing, L. Wang, C. Guo, R. Chen, S. Guo, F. Wu, Energy Environ. Sci. 10 (2017) 1660–1667.
[8] Q. Wang, P. Ping, X. Zhao, G. Chu, J. Sun, C. Chen, J. Power Sources 208 (2012) 210–224.
[9] Z. Cai, Y. Liu, J. Zhao, L. Li, Y. Zhang, J. Zhang, J. Power Sources 202 (2012) 341–346.
[10] H. Rong, M. Xu, L. Xing, W. Li, J. Power Sources 261 (2014) 148–155.
[11] S. Jiang, H. Wu, J. Yin, Z. Wei, J. Wu, L. Wei, D. Gao, X. Xu, Y. Gao, ChemSusChem 14 (2021) 2067–2075.
[12] L. Xia, Y. Xia, Z. Liu, J. Power Sources 278 (2015) 190–196.
[13] J. Feng, L. Lu, J. Power Sources 243 (2013) 29–32.
[14] X. Sun, H.S. Lee, X.Q. Yang, J. McBreen, Electrochem. Solid-State Lett. 5 (2002) 3–7.
[15] L. Xia, S. Lee, Y. Jiang, Y. Xia, G.Z. Chen, Z. Liu, ACS Omega 2 (2017) 8741–8750.
[16] Y. Liu, L. Tan, L. Li, J. Power Sources 221 (2013) 90–96.
[17] H. Rong, M. Xu, B. Xie, X. Liao, W. Huang, L. Xing, W. Li, Electrochim. Acta 147 (2014) 31–39.
[18] X. Zuo, C. Fan, J. Liu, X. Xiao, J. Wu, J. Nan, J. Power Sources 229 (2013) 308–312.
[19] J. Li, L. Xing, R. Zhang, M. Chen, Z. Wang, M. Xu, W. Li, J. Power Sources 285 (2015) 360–366.
[20] X. Liao, P. Sun, M. Xu, L. Xing, Y. Liao, L. Zhang, L. Yu, W. Fan, W. Li, Appl. Energy 175 (2016) 505–511.
[21] Y. Wang, H. Ming, J. Qiu, Z. Yu, M. Li, S. Zhang, Y. Yang, J. Electroanal. Chem. 802 (2017) 8–14.
[22] Q. Liu, G. Yang, S. Liu, M. Han, Z. Wang, L. Chen, ACS Appl. Mater. Interfaces 11 (2019) 17435–17443.
[23] Z. Wang, L. Xing, J.H. Li, M. Xu, W. Li, J. Power Sources 307 (2016) 587–592.
[24] Q. Yu, Z. Chen, L. Xing, D. Chen, H. Rong, Q. Liu, W. Li, Electrochim. Acta 176 (2015) 919–925.
[25] Z. Qin, B. Hong, B. Duan, S. Hong, Y. Chen, Y. Lai, J. Feng, Electrochim. Acta 276 (2018) 412–416.
[26] L. Larush-Asraf, M. Biton, H. Teller, E. Zinigrad, D. Aurbach, J. Power Sources 174 (2007) 400–407.
[27] Y. Wang, L. Xing, X. Tang, X. Li, W. Li, B. Li, W. Huang, H. Zhou, X. Li, RSC Adv. 4 (2014) 33301–33306.
[28] N.P.W. Pieczonka, L. Yang, M.P. Balogh, B.R. Powell, K. Chemelewski, A. Manthiram, S.A. Krachkovskiy, G.R. Goward, M. Liu, J.H. Kim, J. Phys. Chem. C 117 (2013) 22603–22612.
[29] X. Wang, E. Yasukawa, S. Kasuya, J. Electrochem. Soc. 148 (2001) A1058.
[30] X. Wang, E. Yasukawa, S. Kasuya, J. Electrochem. Soc. 148 (2001) A1066.
[31] H. Ota, A. Kominato, W.J. Chun, E. Yasukawa, S. Kasuya, J. Power Sources 119–121 (2003) 393–398.
[32] X. Wang, C. Yamada, H. Naito, G. Segami, K. Kibe, J. Electrochem. Soc. 153 (2006) A135.
[33] H.F. Xiang, H.W. Lin, B. Yin, C.P. Zhang, X.W. Ge, C.H. Chen, J. Power Sources 195 (2010) 335–340.
[34] J. Zhang, J. Wang, J. Yang, Y. Nuli, Electrochim. Acta 117 (2014) 99–104.
[35] H. Rong, M. Xu, B. Xie, W. Huang, X. Liao, L. Xing, W. Li, J. Power Sources 274 (2015) 1155–1161.
[36] G. Yan, X. Li, Z. Wang, H. Guo, C. Wang, J. Power Sources 248 (2014) 1306–1311.
[37] X. Liao, X. Zheng, J. Chen, Z. Huang, M. Xu, L. Xing, Y. Liao, Q. Lu, X. Li, W. Li, Electrochim. Acta 212 (2016) 352–359.
[38] Y. Ren, M. Wang, J. Wang, Y. Cui, Int. J. Electrochem. Sci. 13 (2018) 664–674.
[39] N.N. Sinha, J.C. Burns, J.R. Dahn, J. Electrochem. Soc. 161 (2014) A1084–A1089.
[40] Y.E. Hyung, D.R. Vissers, K. Amine, J. Power Sources 119–121 (2003) 383–387.
[41] D.H. Doughty, E.P. Roth, C.C. Crafts, G. Nagasubramanian, G. Henriksen, K. Amine, J. Power Sources 146 (2005) 116–120.

[42] E.G. Shim, T.H. Nam, J.G. Kim, H.S. Kim, S.I. Moon, J. Power Sources 172 (2007) 919–924.
[43] E.G. Shim, T.H. Nam, J.G. Kim, H.S. Kim, S.I. Moon, J. Power Sources 175 (2008) 533–539.
[44] T. Tsujikawa, K. Yabuta, T. Matsushita, T. Matsushima, K. Hayashi, M. Arakawa, J. Power Sources 189 (2009) 429–434.
[45] Z. Zeng, B. Wu, L. Xiao, X. Jiang, Y. Chen, X. Ai, H. Yang, Y. Cao, J. Power Sources 279 (2015) 6–12.
[46] X. Li, W. Li, L. Chen, Y. Lu, Y. Su, L. Bao, J. Wang, R. Chen, S. Chen, F. Wu, J. Power Sources 378 (2018) 707–716.
[47] K. Xu, M.S. Ding, S. Zhang, J.L. Allen, T.R. Jow, J. Electrochem. Soc. 150 (2003) A161.
[48] M.S. Milien, H. Beyer, W. Beichel, P. Klose, H.A. Gasteiger, B.L. Lucht, I. Krossing, J. Electrochem. Soc. 165 (2018) A2569–A2576.
[49] A. von Cresce, K. Xu, J. Electrochem. Soc. 158 (2011) A337.
[50] G. Yang, J. Shi, C. Shen, S. Wang, L. Xia, H. Hu, H. Luo, Y. Xia, Z. Liu, RSC Adv. 7 (2017) 26052–26059.
[51] M.S. Milien, U. Tottempudi, M. Son, M. Ue, B.L. Lucht, J. Electrochem. Soc. 163 (2016) A1369–A1372.
[52] N. von Aspern, S. Röser, B. Rezaei Rad, P. Murmann, B. Streipert, X. Mönnighoff, S.D. Tillmann, M. Shevchuk, O. Stubbmann-Kazakova, G.V. Röschenthaler, S. Nowak, M. Winter, I. Cekic-Laskovic, J. Fluor. Chem. 198 (2017) 24–33.
[53] J. Kim, V.A.K. Adiraju, N. Rodrigo, J. Hoffmann, M. Payne, B.L. Lucht, ACS Appl. Mater. Interfaces 13 (2021) 22351–22360.
[54] J. Liu, X. Song, L. Zhou, S. Wang, W. Song, W. Liu, H. Long, L. Zhou, H. Wu, C. Feng, Nano Energy 46 (2018) 404–414.
[55] Q.-K. Zhang, X.-Q. Zhang, H. Yuan, J.-Q. Huang, Small Sci. 1 (2021) 2100058.
[56] Y. Zhu, X. Luo, H. Zhi, Y. Liao, L. Xing, M. Xu, X. Liu, K. Xu, W. Li, J. Mater. Chem. A 6 (2018) 10990–11004.
[57] T.H. Nam, E.G. Shim, J.G. Kim, H.S. Kim, S.I. Moon, J. Power Sources 180 (2008) 561–567.
[58] S. Mai, M. Xu, X. Liao, J. Hu, H. Lin, L. Xing, Y. Liao, X. Li, W. Li, Electrochim. Acta 147 (2014) 565–571.
[59] S.S. Zhang, K. Xu, T.R. Jow, J. Power Sources 113 (2003) 166–172.
[60] X.L. Yao, S. Xie, C.H. Chen, Q.S. Wang, J.H. Sun, Y.L. Li, S.X. Lu, J. Power Sources 144 (2005) 170–175.
[61] C. Peebles, R. Sahore, J.A. Gilbert, J.C. Garcia, A. Tornheim, J. Bareño, H. Iddir, C. Liao, D.P. Abraham, J. Electrochem. Soc. 164 (2017) A1579–A1586.
[62] J.G. Han, S.J. Lee, J. Lee, J.S. Kim, K.T. Lee, N.S. Choi, ACS Appl. Mater. Interfaces 7 (2015) 8319–8329.
[63] J. Pires, A. Castets, L. Timperman, J. Santos-Peña, E. Dumont, S. Levasseur, C. Tessier, R. Dedryvère, M. Anouti, J. Power Sources 296 (2015) 413–425.
[64] Z. Zhou, Y. Ma, L. Wang, P. Zuo, X. Cheng, C. Du, G. Yin, Y. Gao, Electrochim. Acta 216 (2016) 44–50.
[65] D.Y. Kim, H. Park, W.I. Choi, B. Roy, J. Seo, I. Park, J.H. Kim, J.H. Park, Y. S. Kang, M. Koh, J. Power Sources 355 (2017) 154–163.
[66] X. Qi, L. Tao, H. Hahn, C. Schultz, D.R. Gallus, X. Cao, S. Nowak, S. Röser, J. Li, I. Cekic-Laskovic, B.R. Rad, M. Winter, RSC Adv. 6 (2016) 38342–38349.
[67] M. He, C.C. Su, C. Peebles, Z. Feng, J.G. Connell, C. Liao, Y. Wang, I.A. Shkrob, Z. Zhang, ACS Appl. Mater. Interfaces 8 (2016) 11450–11458.
[68] G. Xu, S. Huang, Z. Cui, X. Du, X. Wang, D. Lu, X. Shangguan, J. Ma, P. Han, X. Zhou, J. Power Sources 416 (2019) 29–36.
[69] Y.K. Han, J. Yoo, T. Yim, J. Mater. Chem. A 3 (2015) 10900–10909.
[70] Y.K. Han, J. Yoo, T. Yim, Electrochim. Acta 215 (2016) 455–465.
[71] Y.K. Han, J. Yoo, T. Yim, RSC Adv. 7 (2017) 20049–20056.
[72] C. Peebles, J. Garcia, A.P. Tornheim, R. Sahore, J. Bareño, C. Liao, I.A. Shkrob, H. H. Iddir, D.P. Abraham, J. Phys. Chem. C 122 (2018) 9811–9824.
[73] H.-L. Wu, Y.-H. Chong, H.-C. Ong, C.-M. Shu, J. Therm. Anal. Calorim. 147 (2022) 4245–4252.
[74] W. Wahyudi, V. Ladelta, L. Tsetseris, M.M. Alsabban, X. Guo, E. Yengel, H. Faber, B. Adilbekova, A. Seitkhan, A. Emwas, Adv. Funct. Mater. 31 (2021) 2101593.
[75] Y. Liu, D. Lin, Y. Li, G. Chen, A. Pei, O. Nix, Y. Li, Y. Cui, Nat. Commun. 9 (2018) 1–10.
[76] W. Jia, C. Fan, L. Wang, Q. Wang, M. Zhao, A. Zhou, J. Li, ACS Appl. Mater. Interfaces 8 (2016) 15399–15405.
[77] B.D. Adams, E.V. Carino, J.G. Connell, K.S. Han, R. Cao, J. Chen, J. Zheng, Q. Li, K.T. Mueller, W.A. Henderson, J.G. Zhang, Nano Energy 40 (2017) 607–617.
[78] B. Ramasubramanian, M.V. Reddy, K. Zaghib, M. Armand, S. Ramakrishna, Nanomaterials 11 (2021) 2476.
[79] S.S. Zhang, J. Power Sources 162 (2006) 1379–1394.
[80] N.A. Sahalie, A.A. Assegie, W.-N. Su, Z.T. Wondimkun, B.A. Jote, B. Thirumalraj, C.-J. Huang, Y.-W. Yang, B.-J. Hwang, J. Power Sources 437 (2019), 226912.
[81] L.N. Wu, J. Peng, Y.K. Sun, F.M. Han, Y.F. Wen, C.G. Shi, J.J. Fan, L. Huang, J. T. Li, S.G. Sun, ACS Appl. Mater. Interfaces 11 (2019) 18504–18510.
[82] J. Uddin, V.S. Bryantsev, V. Giordani, W. Walker, G.V. Chase, D. Addison, J. Phys. Chem. Lett. 4 (2013) 3760–3765.
[83] S.J. An, J. Li, C. Daniel, D. Mohanty, S. Nagpure, D.L. Wood III, Carbon N. Y. 105 (2016) 52–76.
[84] A. Wang, S. Kadam, H. Li, S. Shi, Y. Qi, NPJ Comput. Mater. 4 (2018) 15.
[85] D. Aurbach, Y. Gofer, M. Ben-Zion, P. Aped, J. Electroanal. Chem. 339 (1992) 451–471.
[86] E. Peled, D.B. Tow, A. Merson, A. Gladkich, L. Burstein, D. Golodnitsky, J. Power Sources 97 (2001) 52–57.
[87] A.M. Andersson, K. Edström, J. Electrochem. Soc. 148 (2001) A1100.
[88] S. Liu, G.R. Li, X.P. Gao, ACS Appl. Mater. Interfaces 8 (2016) 7783–7789.
[89] X. Li, R. Zhao, Y. Fu, A. Manthiram, EScience 1 (2021) 108–123.
[90] P. Li, L. Chen, Z. Wen, D. Zhang, Y. Zhang, N. Zhang, G. Chen, X. Liu, Chem. Eng. J. 433 (2022), 134468.
[91] S. Gu, S.W. Zhang, J. Han, Y. Deng, C. Luo, G. Zhou, Y. He, G. Wei, F. Kang, W. Lv, Q.H. Yang, Adv. Funct. Mater. 31 (2021) 1–8.
[92] N. Piao, S. Liu, B. Zhang, X. Ji, X. Fan, L. Wang, P.F. Wang, T. Jin, S.C. Liou, H. Yang, J. Jiang, K. Xu, M.A. Schroeder, X. He, C. Wang, ACS Energy Lett. 6 (2021) 1839–1848.
[93] R. Mogi, M. Inaba, S.-K. Jeong, Y. Iriyama, T. Abe, Z. Ogumi, J. Electrochem. Soc. 149 (2002) A1578.
[94] R. Chen, F. Wu, L. Li, Y. Guan, X. Qiu, S. Chen, Y. Li, S. Wu, J. Power Sources 172 (2007) 395–403.
[95] H.J. Santner, K.C. Möller, J. Ivančo, M.G. Ramsey, F.P. Netzer, S. Yamaguchi, J. O. Besenhard, M. Winter, J. Power Sources 119–121 (2003) 368–372.
[96] L. El Ouatani, R. Dedryvère, C. Siret, P. Biensan, S. Reynaud, P. Iratçabal, D. Gonbeau, J. Electrochem. Soc. 156 (2009) A103.
[97] E. Krämer, R. Schmitz, S. Passerini, M. Winter, C. Schreiner, Electrochem. Commun. 16 (2012) 41–43.
[98] Y. Watanabe, Y. Yamazaki, K. Yasuda, H. Morimoto, S.I. Tobishima, J. Power Sources 160 (2006) 1375–1380.
[99] M.L. Lee, Y.H. Li, J.W. Yeh, H.C. Shih, J. Power Sources 214 (2012) 251–257.
[100] W. Li, C. Campion, B.L. Lucht, B. Ravdel, J. DiCarlo, K.M. Abraham, J. Electrochem. Soc. 152 (2005) A1361.
[101] Y. Zhuang, F. Du, L. Zhu, H. Cao, H. Dai, J. Adkins, Q. Zhou, J. Zheng, Electrochim. Acta 290 (2018) 220–227.
[102] F. Lindgren, C. Xu, L. Niedzicki, M. Marcinek, T. Gustafsson, F. Björefors, K. Edström, R. Younesi, ACS Appl. Mater. Interfaces 8 (2016) 15758–15766.
[103] C. Xu, S. Renault, M. Ebadi, Z. Wang, E. Björklund, D. Guyomard, D. Brandell, K. Edström, T. Gustafsson, Chem. Mater. 29 (2017) 2254–2263.
[104] Y. Zhu, Y. Li, M. Bettge, D.P. Abraham, Electrochim. Acta 110 (2013) 191–199.
[105] Q.C. Zhuang, J. Li, L.L. Tian, J. Power Sources 222 (2013) 177–183.
[106] W. Lv, C. Zhu, J. Chen, C. Ou, Q. Zhang, S. Zhong, Chem. Eng. J. 418 (2021), 129400.
[107] K.M. Kim, N.V. Ly, J.H. Won, Y.G. Lee, W. Il Cho, J.M. Ko, R.B. Kaner, Electrochim. Acta 136 (2014) 182–188.
[108] J.H. Won, H.S. Lee, L. Hamenu, M. Latifatu, Y.M. Lee, K.M. Kim, J. Oh, W. Il Cho, J.M. Ko, J. Ind. Eng. Chem. 37 (2016) 325–329.
[109] T. Shiga, C.A. Okuda, Y. Kato, H. Kondo, J. Phys. Chem. C 122 (2018) 9738–9745.
[110] A.M. Haregewoin, A.S. Wotango, B.-J. Hwang, Energy Environ. Sci. 9 (2016) 1955–1988.
[111] C.-C. Su, M. He, C. Peebles, L. Zeng, A. Tornheim, C. Liao, L. Zhang, J. Wang, Y. Wang, Z. Zhang, ACS Appl. Mater. Interfaces 9 (2017) 30686–30695.
[112] H. Kim, T.H. Kim, W. Kim, S.S. Park, G. Jeong, ACS Appl. Mater. Interfaces 15 (2023) 9212–9220.
[113] Y. Wang, S. Nakamura, K. Tasaki, P.B. Balbuena, J. Am. Chem. Soc. 124 (2002) 4408–4421.
[114] R. Gauthier, D.S. Hall, T. Taskovic, J.R. Dahn, J. Electrochem. Soc. 166 (2019) A3707.
[115] K. Chatterjee, A.D. Pathak, A. Lakma, C.S. Sharma, K.K. Sahu, A.K. Singh, Sci. Rep. 10 (2020) 9606.
[116] A.D. Pathak, K. Samanta, K.K. Sahu, S. Pati, J. Appl. Electrochem. 51 (2021) 143–154.
[117] Y.-Q. Chen, T.-Y. Chen, W.-D. Hsu, T.-Y. Pan, L.-J. Her, W.-M. Chang, M. Wohlfahrt-Mehrens, H. Yoshitake, C.-C. Chang, J. Power Sources 477 (2020), 228473.
[118] Y. Hu, W. Kong, H. Li, X. Huang, L. Chen, Electrochem. Commun. 6 (2004) 126–131.
[119] J. Han, C. Hwang, S.H. Kim, C. Park, J. Kim, G.Y. Jung, K. Baek, S. Chae, S. J. Kang, J. Cho, Adv. Energy Mater. 10 (2020) 2000563.
[120] W. Huang, L. Xing, Y. Wang, M. Xu, W. Li, F. Xie, S. Xia, J. Power Sources 267 (2014) 560–565.
[121] B. Tong, Z. Song, H. Wan, W. Feng, M. Armand, J. Liu, H. Zhang, Z. Zhou, InfoMat 3 (2021) 1364–1392.
[122] Z. Sun, H. Zhou, X. Luo, Y. Che, W. Li, M. Xu, J. Power Sources 503 (2021), 230033.
[123] T. Hosaka, T. Fukabori, T. Matsuyama, R. Tatara, K. Kubota, S. Komaba, ACS Energy Lett. 6 (2021) 3643–3649.
[124] P. Janssen, R. Schmitz, R. Müller, P. Isken, A. Lex-Balducci, C. Schreiner, M. Winter, I. Cekić-Laković, R. Schmitz, Electrochim. Acta 125 (2014) 101–106.
[125] Y.-X. Huang, Y.-X. Xie, M.-L. Sun, H. Chen, P. Dai, S.-S. Liu, C.-Y. Ouyang, C.-Y. Liu, B.-B. Hu, S.-J. Liao, ACS Sustain. Chem. Eng. 11 (2023) 3760–3768.
[126] T.J. Lee, J. Soon, S. Chae, J.H. Ryu, S.M. Oh, ACS Appl. Mater. Interfaces 11 (2019) 11306–11316.
[127] D.Q. Nguyen, J. Hwang, J.S. Lee, H. Kim, H. Lee, M. Cheong, B. Lee, H.S. Kim, Electrochem. Commun. 9 (2007) 109–114.
[128] H. Wang, D. Sun, X. Li, W. Ge, B. Deng, M. Qu, G. Peng, Electrochim. Acta 254 (2017) 112–122.
[129] C. Korepp, W. Kern, E.A. Lanzer, P.R. Raimann, J.O. Besenhard, M.H. Yang, K.-C. Möller, D.-T. Shieh, M. Winter, J. Power Sources 174 (2007) 387–393.
[130] M. Xu, L. Zhou, Y. Dong, Y. Chen, J. Demeaux, A.D. MacIntosh, A. Garsuch, B. L. Lucht, Energy Environ. Sci. 9 (2016) 1308–1319.
[131] D. Diddens, W.A. Appiah, Y. Mabrouk, A. Heuer, T. Vegge, A. Bhowmik, Adv. Mater. Interfaces 9 (2022) 2101734.
[132] C. Lv, X. Zhou, L. Zhong, C. Yan, M. Srinivasan, Z.W. Seh, C. Liu, H. Pan, S. Li, Y. Wen, Adv. Mater. 34 (2022) 2101474.
[133] L.D. Ellis, S. Buteau, S.G. Hames, L.M. Thompson, D.S. Hall, J.R. Dahn, J. Electrochem. Soc. 165 (2018) A256.

[134] M. Aykol, P. Herring, A. Anapolsky, Nat. Rev. Mater. 5 (2020) 725–727.
[135] T. Würger, L. Wang, D. Snihirova, M. Deng, S.V. Lamaka, D.A. Winkler, D. Höche, M.L. Zheludkevich, R.H. Meißner, C. Feiler, J. Mater. Chem. A 10 (2022) 21672–21682.
[136] A. Kilic, D. Eroglu, R. Yildirim, J. Electrochem. Soc. 168 (2021) 90544.
[137] X. Qu, A. Jain, N.N. Rajput, L. Cheng, Y. Zhang, S.P. Ong, M. Brafman, E. Maginn, L.A. Curtiss, K.A. Persson, Comput. Mater. Sci. 103 (2015) 56–67.
[138] F. Hildenbrand, F. Aupperle, G. Stahl, E. Figgmeier, D.U. Sauer, Batter. Supercaps 5 (2022), e202200038.
[139] T.N. Tran, A. Garg, T.G. Phung, M.L.P. Le, N.G. Panwar, J. Energy Storage 42 (2021), 103012.